Separation of distinct exosome subpopulations: isolation and characterization approaches and their associated challenges

Karishma Singh,†[a] Ruchika Nalabotala,†[a] Kevin M. Koo, [ID] *[b] Sudeep Bose,[c] Ranu Nayak [ID] *[a] and Muhammad J. A. Shiddiky [ID] *[d]

Exosomes are nano-sized extracellular vesicles that serve as a communications system between cells and have shown tremendous promise as liquid biopsy biomarkers in diagnostic, prognostic, and even therapeutic use in different human diseases. Due to the natural heterogeneity of exosomes, there is a need to separate exosomes into distinct biophysical and/or biochemical subpopulations to enable full interrogation of exosome biology and function prior to the possibility of clinical translation. Currently, there exists a multitude of different exosome isolation and characterization approaches which can, in limited capacity, separate exosomes based on biophysical and/or biochemical characteristics. While notable reviews in recent years have reviewed these approaches for bulk exosome sorting, we herein present a comprehensive overview of various conventional technologies and modern microfluidic and nanotechnological advancements towards isolation and characterization of exosome subpopulations. The benefits and limitations of these different technologies to improve their use for distinct exosome subpopulations in clinical practices are also discussed. Furthermore, an overview of the most commonly encountered technical and biological challenges for effective separation of exosome subpopulations is presented.

1. Introduction

Exosomes are extracellular lipid membrane nanovesicles which mediate intercellular communication as well as eradication of cellular garbage. In the past decade, exosomes have generated significant interest among the scientific research community due to the potential of being a biological information reservoir. Exosomes carry cargo proteins, nucleic acids or lipids from mother cells to distant recipient cells through bodily fluids during intercellular communication and signaling.[1] This makes exosome separation crucial for both diagnostic and therapeutic purposes in various diseases;[2,3] including cancer, infectious diseases, cardiovascular diseases, or neurodegenerative diseases.[4–6]

[a]*Amity Institute of Nanotechnology, Amity University Uttar Pradesh, Noida 201301, UP, India. E-mail: rnayak@amity.edu*
[b]*The University of Queensland Centre for Clinical Research (UQCCR), Herston, QLD 4029, Australia. E-mail: maisheng.koo@uqconnect.edu.au*
[c]*Amity Institute of Biotechnology, Amity University Uttar Pradesh, Noida 201301, UP, India*
[d]*School of Environment and Natural Sciences and Queensland Micro- and Nanotechnology Centre, Griffith University, Nathan, QLD 4111, Australia. E-mail: m.shiddiky@griffith.edu.au*
†Authors contributed equally.

There is increasing evidence that exosomes are highly heterogeneous to be able to mediate a wide spectrum of effects on recipient cells and this heterogeneity further complicates the challenge of exosome separation from biofluid samples. It is now widely accepted that exosomes consist of distinct exosome subpopulations which utilize different biophysical (*e.g.* size, zeta potential, stiffness) and biochemical (*e.g.* surface expression, molecular cargo) properties to mediate different effects on recipient cells.[7–9] Interestingly, it has been noted that several exosome isolation methods have indicated the presence of distinct exosome subpopulations from a heterogeneous starting sample.[10–12] It must be noted that isolation methods enabling enriched separation as well as post-isolation characterization techniques of distinct exosome subpopulations are equally important.[13,14] The combination of stringent exosome isolation and characterization is ideal for addressing the complexities of heterogeneous exosome subpopulations, thereby granting clarity in the specific biological roles of various exosome subpopulations.

The lack of an efficient standardized exosome isolation method is the foremost challenge for resolving exosome subpopulation analysis. It has been reported that exosomes can be isolated by individual or combinations of different well-known methods; including ultracentrifugation, size exclusion, or immunoaffinity capture techniques.[15,16] Each of these

methods target a specific characteristic of exosomes (such as size or surface protein expression) and has its own inherent benefits for exosome subpopulation isolation. In addition to these existing techniques, there have been a huge influx of innovative exosome isolation techniques which leverage technological advances in modern fields of microfluidics or magnetic nanomaterials.

Post-isolation, it is crucial that isolated exosome subpopulations can be characterized both biophysically and biologically to accurately sort out distinct exosome subpopulations. Conventional characterization techniques include enzyme-linked immunosorbent assay (ELISA), western blotting, flow cytometry for immuno-characterization; as well as nanoparticle tracking analysis (NTA), tunable resistive pulse sensing (TRPS) for characterization of exosome biophysical attributes.

Despite several reviews on exosome isolation and detection techniques,[7,17,18] a focused take on the requirements for separating distinct exosome subpopulations is yet to be summarized. In a bid to address this crucial point, we herein provide a comprehensive overview of various conventional technologies and modern microfluidic and nanotechnological advancements towards isolation and characterization of exosome subpopulation (Fig. 1). It is critical to understand the benefits and limitations of these different technologies as this may bring about more innovations in near future to improve the use of distinct exosome subpopulations in clinical practices. We also enumerate the technical and biological challenges that is currently impeding effective separation of exosome subpopulations.

2. Exosome isolation methods

Exosomes have been demonstrated to be very promising disease biomarkers and therapeutic agents,[19–22] and various isolation methods have been developed to separate these nano-sized extracellular vesicles which are spread intricately throughout various body fluids.[23] The most common exosome isolation techniques typically exploit the unique biophysical or biochemical properties of exosomes (Table 1) and can be categorized into different methodology classes such as ultracentrifugation, ultrafiltration, immunoaffinity, or precipitation. Additionally, there have also been modern microfluidics and nanomaterial innovations for enhanced exosome isolation.

2.1. Ultracentrifugation

Ultracentrifugation is the most commonly used method for biophysical-based isolation of exosomes as it offers an easy operation protocol with minimal preparation of starting samples and involves basic technical know-how to perform.[17,23–26] The centrifugal force involved in ultracentrifugation mostly ranges around $100\,000g$ relative centrifugal force. The plasma or serum samples used for exosome isolation is generally first prepared before a multi-step ultracentrifugation step is conducted. This preparation step is performed by removing the bulky non-target biomolecules and integrating protease blockers which restrict the degradation of the exosomal proteins.[27] The centrifugal force is increased with each successive multi-step ultracentrifugation runs and the exosomes procured in the final run can be stored in sub-zero temperatures or precisely at -80 °C before downstream analysis.[17]

Another form of ultracentrifugation is density-gradient ultracentrifugation whereby a sucrose density gradient is used during ultracentrifugation. It has been reported that the concentration of the obtained exosomes by density-gradient ultracentrifugation was increased by three times as compared to ultracentrifugation without the use of a density gradient.[26,28,29] In addition, iso-osmotic gradients such as non-ionic iodixanol could be included to retain the structure of the exosomes during ultracentrifugation.[30]

The downsides of ultracentrifugation are that it is a prolonged process with multiple ultracentrifugation runs, requires a high volume of starting sample, and needs ultracentrifugation equipment which are not transportable.[23,24]

2.2. Size-based isolation

2.2.1. Ultrafiltration. Ultrafiltration of exosomes is the most typical size-based technique which uses the principle of basic filtration; where a permeable/filtering membrane (size ranging between 30–200 nm) is used to separate particles based on their size and molecular weight. The filtering membrane is generally made of polycarbonate etched nanoporous membrane or ether sulfone membrane.[31,32] During ultrafiltration of samples, the biomolecules which are greater than the molecular weight cut off (MWCO) gets collected on the surface of the membrane and the biomolecules (*i.e.* exosomes) smaller than the MWCO pass through the filtering membrane into the filtrate.[17] As compared to ultracentrifugation, ultrafiltration is a fast exosome isolation process with low equipment cost and easily can eliminate large cellular debris and dead cells which are greater in size.[33]

The ultrafiltration workflow for exosome isolation is also available as commercial kits. For example, a company in USA called 'Bioo Scientific' – part of PerkinElmer – has developed
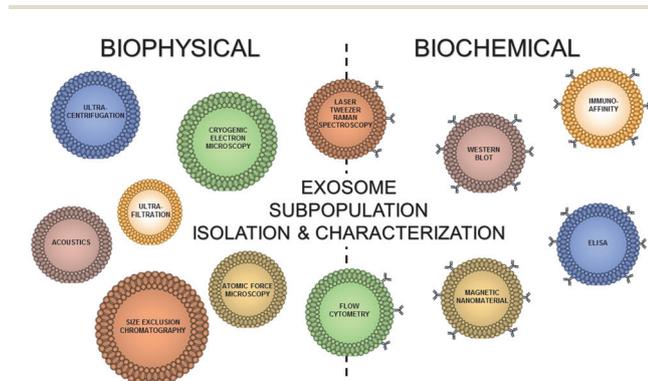
Fig. 1 Different conventional and modern technologies towards biophysical and/or biochemical isolation and characterization of distinct exosome subpopulations.

Table 1 Summary of different exosome isolation methods

Technique	Working principle	Biophysical/biochemical properties	Benefits	Disadvantages
Ultracentrifugation	Separation of molecules based on relative centrifugal forces of around 100 000g	• Biophysical separation range of around 50–250 nm-sized particles • Separation based on size and molecular weight	• Easy operation protocol • Minimal preparation of staring samples • Basic technical know-how	• Prolonged process with multiple runs • High volume of starting samples • Bulky equipment • Possible mechanical damage of exosomes
Ultrafiltration	Segregation of particles through a permeable membrane	• Biophysical separation range of around 50–250 nm-sized particles • Separation based on size and molecular weight	• No elaborate instrumentation needed • Rapid workflow	• Tendency of clogging on the filtering membrane • Potential exosome deformation and lysis due to transmembrane pressure
Size exclusion chromatography	Isolation of nanovesicles through a column with porous stationary phase in which small particles can penetrate	• Biophysical separation range of around 50–250 nm-sized particles • Separation based on size	• Preserves the biological activity, vesicle structure of nanovesicles	• Not easily scalable for high throughput • Time-consuming procedure
Asymmetrical flow field-flow fractionation	Sample is put through a parabolic flow and a flow which is perpendicular to the parabolic flow generates the separation of nanovesicles	• Biophysical separation range of few nm to µm • Separation based on size and molecular weight	• Broad range of nanovesicle size separation • Uniform exosome populations can be obtained at high throughput	• Expensive • Time-consuming procedure • Possible poor sample recovery yield
Immunoaffinity	Antibodies are used to capture exosomes based on surface antigen expression	• Biochemical separation based on binding to membrane proteins on exosomes (*e.g.* CD63)	• High specificity • Good purity	• Limited by antibody specificity • Antigen used must be expressed on the exosome surface • Expensive procedure • Low yield
Acoustics	Microfluidics-based isolation system whereby vesicles are separated based on exposure to ultrasound waves	• Biophysical separation range of 30–200 nm • Separation based on size	• Rapid and simple procedure	• Technique efficacy is greatly affected by environmental factors
Sieving	Microfluidics-based technique where samples are directly filtered through nanoporous membranes using pressure or electrophoresis	• Biophysical separation range of 30–180 nm • Separation based on size	• No sample pre-treatment • Eliminates interfering soluble proteins • High yield and purity	• Possibility of clogging and causing instrumental damage
Magnetic nanomaterials	Antibody/aptamer-conjugated magnetic surfaces enable separation of exosomes in magnetic capture setup	• Biochemical separation based on binding of antibodies on magnetic nanomaterial surface to membrane proteins on exosomes (*e.g.* CD63)	• Low cost • Stable colloidal suspension (negligible magnetic moment without external magnetic field) • Easy surface biofunctionalization • High surface-to-volume ratio for high exosome isolation yield	• Technical challenges in nanomaterial synthesis

an isolation kit known as 'ExoMir'. These commercially available kits usually use pretreated samples which are passed through modified syringes with filters. As the sample passes through, extracellular vesicles greater than approximately 200 nm get retained in the first filter; and vesicles which size ranges between 20–200 nm get collected on the second filter, and only the smallest vesicles (smaller than 20 nm) are filtered out.[25,34]

In the ultrafiltration procedure, membrane clogging is a key challenge which can lead to exosomes being trapped in the clogged filters. This will result in low exosome isolation yield and high isolation bias of exosome subpopulations.[17,24]

2.2.2. Size exclusion chromatography. Size exclusion chromatography is first based on the principle of using a column made of starch and water to separate solutes of

various molecular weights when passing through an aqueous medium.[23] In this technique, a column is fitted with a porous stationary phase where biomolecules smaller than the pores within the column can penetrate,[25] but is slowed down because of trapping inside the pores. The larger biomolecules are incapable of entering the pores due to obstruction by the smaller biomolecules and hence are removed by washing.[23] Over the years, size exclusion chromatography has been developed for effective exosome isolation and offers various advantages such as compatibility with various types of biofluids, requirement of very small sample volumes, and post-isolated retainment of intact exosome structures.[23,35,36] There have also been innovations in column composition made of agarose dextran or hydrophilic synthetic polymers to enable better performance. Size exclusion chromatography is traditionally not easily scalable and highly challenging for high throughput exosome isolation applications[37] but still ranks highly as a commonly utilized exosome isolation technique.

2.2.3. Asymmetrical flow field-flow fractionation. Asymmetrical flow field-flow fractionation (AF4) is a sub-class of field-flow fractionation techniques. It separates particles according to their diffusion coefficient. Separation is achieved in a channel consisting of two plates separated by a spacer.[38,39] The upper plate is impermeable, whereas the bottom plate is permeable and made of a porous frit covered by a semipermeable membrane with a defined pore-size. A high-resolution separation is achieved within the parabolic flow profile passing through the channel, against which a perpendicular cross-flow is applied. The particles are driven by the cross-flow toward the channel bottom plate or accumulation wall. However, because of the counteracting Brownian motion of the particles, an equilibrium position is reached away from the accumulation wall. Small particles with high diffusion coefficient float closer to the channel center and are displaced by the faster flow stream of the parabolic flow profile. Thus, smaller particles elute earlier than larger particles with smaller diffusion coefficient, which drives them closer to the accumulation wall where the flow is slower. The availability of AF4 is less and it is expensive as compared to other techniques. However, AF4 system covers a broad separation range from nm to μm and is thus suitable for exosome separation.[40]

2.3. Immunoaffinity capture

Exosomes possess a number of specific receptors and proteins such as CD9, CD63, CD81 on their membrane surfaces[17,24,33] and this gives us opportunities to develop highly specific isolation *via* immunoaffinity. A major benefit of immunoaffinity isolation is that it allows for distinct exosome subpopulation sorting (with different surface protein expression) as it is based on selective antibody–antigen binding.[25]

For immunoaffinity capture, antibodies targeting a particular antigen are typically adhered to solid support surfaces such as within microfluidic channels (discussed in latter sections) or on magnetic beads.[25,41–43] Although highly specific, immunoaffinity capture has drawbacks of needing pre-requisite

knowledge of targeted antibody–antigen interactions, and for antigens to be present on the exosome surface for higher likelihood of antibody binding. For efficient separation of distinct exosome subpopulations, the yield of immunoaffinity exosome isolation can be further improved by coupling with ultrafiltration or ultracentrifugation methods.

2.4. Microfluidics

Microfluidics is the technology of manipulating small amount of fluids ranging between 10^{-6} to 10^{-15} L within micron-sized channels. The advantages of using microfluidics technology include portability,[44] reconfigurability, high throughput,[45,46] and automation.[47–49] To date, the microfluidics technologies for exosome isolation methods are based on immunoaffinity capture, acoustics, sieving, and nanomaterials. Being a unique miniaturized separation technique for separation of exosomes, the advancements in microfluidics technology can significantly push the boundaries of exosome separation science.

2.4.1. Immunoaffinity. The underlying principle of immunoaffinity is based on the binding interactions between the exosome surface membrane-bound proteins and the immobilized antibodies on the surface of a microfluidic device.[50] Using the immobilized antibodies on the higher surface area ratio of the microfluidic device aids in intensifying exosome binding interactions from small sample volumes and obtaining higher isolation yields.

Irimia *et al.* fabricated a microfluidic device with herringbone grooves and demonstrated the processing of up to 400 μL of sample volume for vesicle isolation.[51] Often, microfluidic devices for exosome isolation are made using polydimethyl siloxane (PDMS) that are functionalized with antibodies on the inner surface of the channels.[52,53] PDMS is a preferred material for fabricating flexible microfluidic devices due to its unique rheological properties.[54] Additionally, novel surface modification strategies for PDMS enable changes from hydrophobic to hydrophilic state[55] to transform surface wettability and remove limitations on fluid flow.

Oosterkamp and colleagues demonstrated a unique microfluidic device with removable microfluidic tracts on a modified surface of mica. The device showed an increase in the concentration of the trapped exosomes when examined by atomic force microscopy.[56] Microfluidic devices which incorporated graphene oxide nanostructures and polydopamine nanostructures on the inner device surfaces have also displayed increased exosome isolation ability.[57–59]

Microfluidic exosome analysis platforms have been developed where an anti-CD63 functionalized channel was used for immuno-capturing of exosomes from human serum.[60] The anti-CD63 functionalized channel was also used by Nagrath *et al.* in another method, referred to as the *ExoChip*. The *ExoChip* method utilized a surface-functionalized circular microchamber to capture exosomes, followed by fluorescent carbocyanine dye staining for quantification.[61] Godwin *et al.* developed a device that enables on-chip immuno-isolation and *in situ* detection of exosomes directly from patient plasma. In this method, isolation and enrichment of circulating

exosomes, on-line chemical lysis, protein immunoprecipitation, and sandwich immunoassays were performed on a single chip before chemifluorescence detection. The device (Fig. 2a) was successfully tested for exosome isolation and analysis in plasma specimens derived from lung cancer patients.[62]

Recently, another microfluidic device (Fig. 2b) was reported by Liu and colleagues which the sample was first premixed with a capture agent Mag-CD63 to form Mag-CD63-Exo com-plexes.[63] The complexes were then passed through inlet 1, while the primary antibodies were introduced through inlet 2. This allowed the formation of Mag-CD63-Exo-Ab1 complexes. Then, the fluorescently labelled secondary antibodies were introduced through inlet 3 to capture the target exosomes, which were finally examined by an inverted fluorescence microscope. This on-chip sensor was challenged to capture breast cancer specific exosomes in clinical samples, and the results showed that a significantly higher number of EpCAM-
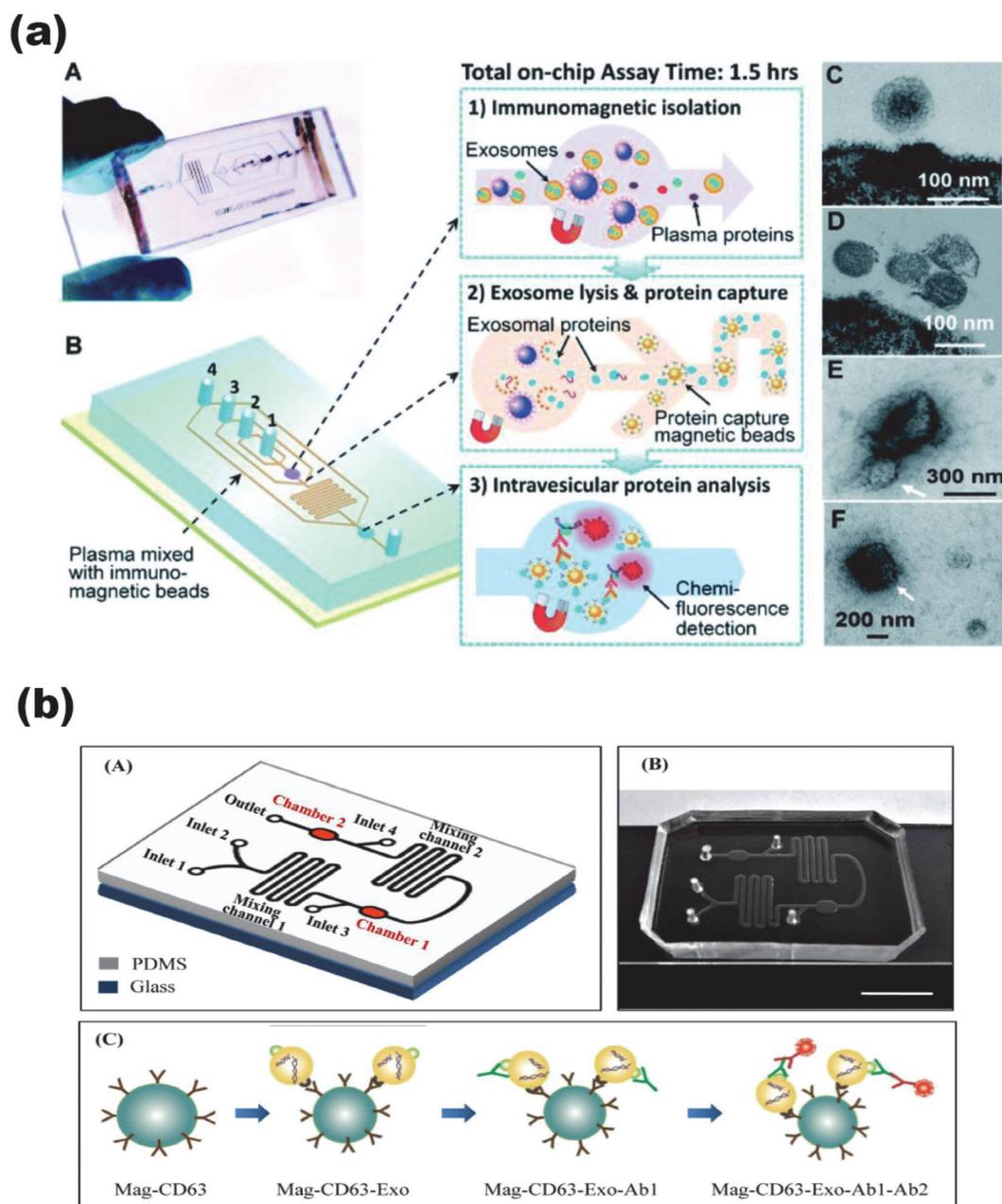
Fig. 2   (a) Integrated microfluidic exosome isolation and analysis directly from human plasma. (A) Image of the prototype PDMS chip containing a cascading microchannel network for multi-stage exosome analysis. (B) Streamlined workflow for on-chip immunomagnetic isolation, chemical lysis, and intravesicular protein analysis of circulating exosomes. Adapted from ref. 62 with permission from Royal Society of Chemistry, Copyright 2014. (b) Device design and principle for immunomagnetic exosome isolation and detection. (A) Schematic representation of the microfluidic device. (B) Image of the device. The scale bar represents 1 cm. (C) On-device exosome isolation and detection workflow. Adapted from ref. 63 with permission from PLOS, Copyright 2017.

positive exosomes were present in the plasma of breast cancer patients than in healthy controls.

Castro and colleagues have developed an immuno-magnetic exosome RNA (iMER) microfluidic platform for on-chip enrichment, purification, and analysis of exosomal RNA. The *iMER* uses magnetic beads with anti-EGFR/EGFRvIII coating to isolate and enrich cancer-specific exosomes. The enriched and isolated subpopulations of exosomes are lysed in the chip and introduced to a glass bead filter. Next, mRNA in the exosomes are absorbed onto a glass bead *via* electrostatic interaction between the glass substrate and mRNAs. The isolated mRNAs were then reverse transcribed, amplified, and measured by qPCR.[64]

2.4.2. Acoustics. The integration of acoustics and microfluidic is termed as "*acoustofluidics*" and it offers a label-free approach of exosome separation by using radiation forces on biomolecules which are present in the biofluid sample.[65,66] *Acoustofluidics* is based on the synergy between the acoustic waves with the biofluids and composition inside the biofluids.[67,68] The beneficial way of generating the acoustic waves is by using piezoelectric material-based transducers. This material is a suitable choice because under mechanical stress, they can generate electrical polarization.[69,70] Materials like quartz have piezoelectric property naturally because of its crystal structure which gains a net electric dipole. In this type of microfluidic based isolation technique, exosomes are separated from the matrix along with other extracellular vesicles based on their sizes. The matrix containing the exosomes and other cellular components is inserted into a chamber and subjected to ultrasound waves. The ultrasound waves apply radiation forces on the biomolecules, and the response of the biomolecules to the applied force is dependent on their size and density. The bigger biomolecules will experience a larger radiation force and therefore move faster.[71] In this *acoustofluidics* method, the risk of channel clogging is highly minimized because the filtration is carried out continuously.

Lee *et al.* used a pair of interdigital transducer (IDT) electrodes as an ultrasound source to generate surface acoustic waves (SAW). This *acoustofluidics* effect deflected the larger biomolecules in a sample to their outlets on the side of the microfluidic device (Fig. 3a) and isolated extracellular vesicles smaller than 200 nm.[71] This technique has many advantages: (a) easy fabrication and simple to integrate with microfluidic devices, (b) biocompatibility, (c) biomolecule manipulation without any physical contact, (d) rapid fluidic activation.[72–74] Although *acoustofluidics* can offer size-based sorting of distinct exosome subpopulations, it is expected that integrating this technique with immunoaffinity methods would be helpful for further exosome subpopulation immunoprofiling.[75]

2.4.3. Sieving. It would be highly desirable if exosomes can be extracted directly from the complex biofluids like blood, since it would omit any pre-treatment of the biofluid sample. Park and colleagues experimentally showed an innovative microfluidics method of exosome isolation by filtering whole blood through a membrane driven by either pressure or electrophoresis.[76] The microfluidic device was prepared with an adjustable nanoporous membrane which was permeable to small extracellular vesicles but removed large cells and other cellular debris. The pressure-driven method had a higher isolation yield but was limited by channel clogging; whereas the electrophoresis-driven method observed no clogging and ensured high exosome purity by eliminating interfering soluble proteins.

Several microfluidic exosome isolation platforms have been demonstrated based on the size exclusion technique. For example, nanoporous membranes have been fabricated in a microfluidic filtration system to isolate nanovesicles from whole blood with a tunable size cut-off. More recently, advanced microfluidic sieving methods for isolating exosomes have been reported.[77,78] In this double-filtration microfluidic device, a primary membrane with a pore size of 200 nm removed larger extracellular vesicles and impurities from urine and a secondary membrane with a pore size of 30 nm isolated the smaller exosomes.[77] Microfluidic sieving can achieve a high exosome isolation yield ranging from 30–200 nm in size.

2.4.4. Nanomaterials. Microfluidic devices can be integrated with nanomaterials for effective exosome isolation. Zhu *et al.* designed a bio-inspired NanoVilli chip for highly efficient isolation of non-small cell lung cancer-derived nanovesicles.[79] The NanoVilli structures were constructed from silicon nanowire arrays and bio-inspired by the distinctive structures of intestinal microvilli which are densely packed on the intestinal walls for increased surface areas. After immuno-capturing of target nanovesicles on the NanoVilli nanomaterial, RNA was collected for the downstream reverse transcription digital droplet PCR analysis.

The same research group has more recently demonstrated an extracellular vesicle-Click Chip (Fig. 3b) which synergistically integrated covalent click chemistry-mediated extracellular vesicle capture/release, multimarker antibody cocktails, nanostructured substrates, and microfluidic chaotic mixers. The Click Chip similarly employs the use of densely packed silicon nanowires substrates which dramatically increases the capture surface area in contact with extracellular vesicles. Moreover, the microfluidic chaotic mixer (made of polydimethylsiloxane) facilitates repeated physical contact between silicon nanowires and the flow-through extracellular vesicles, further enhancing the capture performance. After click chemistry-mediated capture, 1,4-dithiothreitol (DTT) is used as a disulfide cleavage agent to promptly release the captured extracellular vesicles by breaking the embedded disulfide bonds. Importantly, the Click Chip has now been demonstrated for isolation of intact tumor-derived extracellular vesicles in sarcoma[80] and hepatocellular carcinoma[81] for functional downstream analyses.

Liu *et al.* developed an innovative method for exosome isolation whereby porous silicon nanowires were formed on micropillar structures in a ciliated fashion for trapping exosomes on a microfluidic device.[82] The porous silicon nanowires were patterned onto the sidewalls of the micropillars by combining electroplating, microfabrication and metal assisted nanowire etching. These nanostructures preferentially cap-
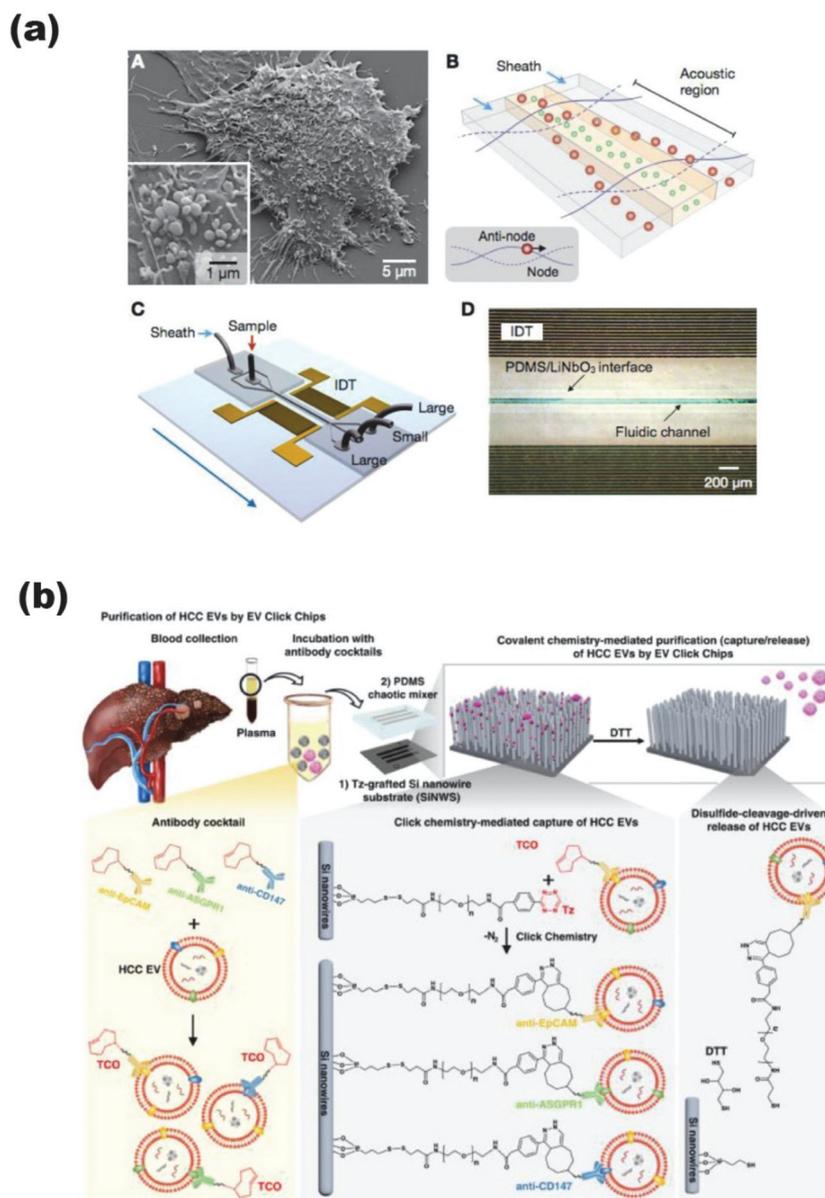
Fig. 3 (a) Acoustic isolation of nanovesicles. (A) Scanning electron microscopy image of isolated nanovesicles. (B) Nanovesicles under acoustic radiation pressure are transported to nodes of acoustic pressure region (inset). (C) A pair of interdigitated transducer electrodes are used to generate a standing surface acoustic wave across the flow direction. (D) Micrographs of the device. Adapted from ref. 71 with permission from American Chemical Society, Copyright 2015. (b) Schematic illustration of the device configuration and working mechanism of a Click Chip, which uniquely integrates several coherent strategies including covalent chemistry-mediated nanovesicle capture/release, a multimarker antibody cocktail, nanostructured substrates, and a polydimethylsiloxane-based chaotic mixer, promising rapid and effective purification of intact extracellular vesicles. Adapted from ref. 81 with permission from Springer Nature, Copyright 2020.

tured exosome nanovesicles between the interstitial sites of the nanowires, and the trapped exosomes can be recovered with high purity by dissolving these silicon nanowires in buffer.[82] The combined use of microfluidics and nanomaterials is advantageous for efficient and high isolation of exosomes, but several barriers remain to be overcome in terms of nanomaterial dimension optimization, stability, and reproducible synthesis.

2.5. Magnetic nanomaterials

Magnetic nanomaterial-based separation of exosomes has gained a lot of popularity because of their elevated levels of biocompatibility with remarkable biotarget isolation and detection properties.[83–86] In general, magnetic nanomaterials have displayed notable benefits in disease and diagnostic applications because they can be used as direct capture

vehicles or carriers of desired biological probes.[87–89] Recently, magnetic properties of superparamagnetic particles have been used as detection and signal-amplifying tools in various biosensing platforms.[9,90] Examples of magnetic nanomaterials include superparamagnetic iron oxide nanoparticles; ferrites of nickel, gold, manganese and cobalt; that are particularly gaining popularity for their plethora of characteristics.[85,86,91] Lately, these magnetic nanomaterials have been utilized for simple and effective ways of exosome isolation.

2.5.1. Iron oxide nanoparticles. In developing a novel exosome isolation technique, Yu *et al.* synthesized iron oxide nanoparticles and coated them with polyethylene glycol (PEG) using chemical co-precipitation method to yield nanoparticles of approximately 10 nm in radius.[92] Using the PEG-coated iron oxide nanoparticles, exosomes in fetal bovine serum (FBS) were successfully captured and precipitated using a magnet. The results showed that the proteins in the FBS were reduced to up to 40% of the original amount and the exosomes remained intact.[92]

Wong and co-workers designed electrochemical biosensor with magnetic isolation for exosomes present in saliva.[93] Anti-CD63-based streptavidin-coated magnetic beads was used for rapid and effective capturing of exosomes. Most reported iron oxide superparamagnetic nanoparticle-based exosome isolation are demonstrated on antiCD63 which narrow the varied range of exosome subpopulations. As a result, a new magneto-immunosensor (Fig. 4a) was introduced based on combination of antibodies for overcoming this drawback for overcoming this drawback of only using CD63.[94] Exosomes were first magnetically isolated with magnetic beads using generic tetraspanin antibody (*e.g.* CD63 or CD9) and labelled with CdSe quantum dots that were conjugated with biotinylated FAM134B and HER-2 antibodies. For the first time, quantum dots were used as signal amplifier agent in anodic stripping voltammetry measurement for the sensitivity improvement.

Additionally, it has been discovered that several superparamagnetic nanoparticles, especially magnetic ferric oxide-containing nanoparticles, exhibit natural enzymatic activity. For example, iron oxide nanoparticles were employed as a signal enhancing element for the electrochemical immunosensing of carcinoembryonic antigen (CEA). An external magnet could be used with subsequent magnetic purification to make the sensor reproducible and reusable.[95,96] A similar sandwich-type immunoassay has been reported for ultrasensitive detection of the carbohydrate antigen (CA-125) and AFP based on the magnetic nanoparticles as a signal amplifier.[97]

2.5.2. Gold-loaded ferric oxide nanocubes. It has been found that superparamagnetic iron oxide nanoparticles have horseradish peroxidase-mimicking property towards the oxidation of chromogenic substances like tetramethylbenzidine.[98,99] Shiddiky *et al.* engineered superparamagnetic gold-loaded ferric oxide nanocubes for isolating exosomes directly from bodily fluids.[86] These gold-loaded ferric oxide nanocubes are highly porous and allow for the direct attachment of many bioaffinity probes to drastically improve exosome capturing efficiency. The superparamagnetic gold
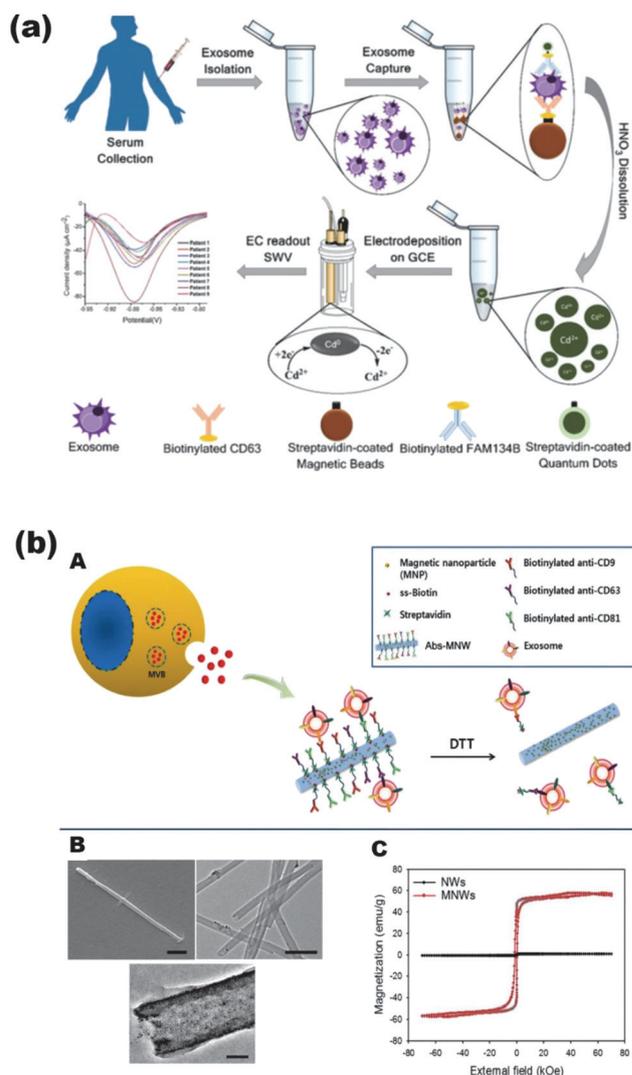
Fig. 4 (a) Magnetic bead assay for the isolation and detection of disease-specific exosomes. Bulk exosome populations were initially magnetically isolated by a generic antibody (CD63 or CD9) followed by the isolation of cancer-specific exosomes using CdSeQD-functionalized specific antibody (FAM134B or HER2). After magnetic washing and purification steps, anodic stripping voltammetric quantification of Cd2+ were carried out to quantify the disease-specific exosomes. Adapted from ref. 94 with permission from Royal Society of Chemistry, Copyright 2017. (b) (A) Antibody cocktail-conjugated magnetic nanowires for the isolation of exosomes. (B) Scanning electron microscopy (left: scale bar, 500 nm) and transmission electron microscopy (right: scale bar, 500 nm and bottom: scale bar, 100 nm) imaging of antibody-conjugated magnetic nanowires. (C) Magnetic hysteresis loop of magnetic nanowires (MNWs) and bare nanowires (NWs) at room temperature. Adapted from ref. 101 with permission from Springer Nature, Copyright 2019.

loaded ferric oxide nanocubes were functionalized with an exosome-associated antibody (CD63) as a first step and later dispersed in the biofluid sample to capture the exosomes present in the sample for magnetic isolation.[86] In all, the multifunctionality of these superparamagnetic ferric oxide nanocubes can (a) promote electrocatalysis, (b) act as a capture

agent, and (c) serve as nanozymes to detect both miRNA and autoantibody biomarkers.[86]

2.5.3. Magnetic nanowires. Alonso and co-workers developed a method to isolate tumor derived exosomes (TEX) using hybrid magnetic nanowires of iron and gold.[100] Different concentrations of iron/gold magnetic nanowires were added to 3×10^5 cells. It was postulated that the magnetic nanowires were packed into TEX and provided a medium to be isolated by a magnetic stand. After characterization by nanoparticle tracking analysis, it was concluded that the isolated TEX by magnetic iron/gold nanowires provided an almost equivalent size distribution in a fast yet cost effective way.[100] As compared to similar iron/gold magnetic nanomaterials with different shapes and sizes, the iron/gold nanowires are synthesized by electrodeposition, thus making their structure and magnetic response easily tunable according to the specific applications (such as enhanced blood circulation and tumor internalization).

Cho and colleagues described the use of antibody cocktail-conjugated magnetic polypyrrole nanowires (Fig. 4b) to isolate tumor-derived exosomes from the plasma samples of cancer patients.[101] The elongated polypyrrole nanowires were doped with magnetic nanoparticles and biotin moieties for conjugation with diverse exosome-specific antibodies such as anti-CD9, anti-CD63 and anti-CD81. The elongated morphology of the magnetic polypyrrole nanowires offered more flexibility and versatility for exosome isolation by facilitating multiple interactions through the recognition receptors, resulting in enhanced target exosome isolation from small volume samples. The same research group has also proposed the use of conductive polypyrrole nanowires for direct and efficient isolation of exosomes.[102] Although not technically a magnetic-based isolation principle, the conductive polypyrrole nanowires can isolate target exosomes for finely controlled retrieval in a similar fashion by using electrical- or glutathione-mediated stimulation. The three-dimensional surface of the polypyrrole nanowires have nano-topographic structures that allow the specific isolation of nanosized exosomes by promoting topographical interactions, while physically blocking larger mircrovesicles. In addition, the vertically aligned features significantly improve isolation efficiency after modification with desired target-binding antibodies. The polypyrrole nanowires were synthesized electrochemically and the surfaces were conjugated with antibodies that recognized proteins on the surface of the exosomes (i.e., anti-CD9, anti-CD63, antiCD-81).[102]

Magnetic nanowires made of nickel are often synthesized by electrodeposition on porous alumina templates. Nickel nanowires can be used to develop quick, efficient, and cost-effective methods for isolating tumor derived exosomes. The elongated structure of the magnetic nickel nanowires with high aspect ratio showed a very high efficiency of the isolation of exosomes. The magnetic nickel nanowires can be incubated with cancer cells and then encapsulated into endosomes in the cells. When released into the culture medium, the nickel nanowires get attached to tumor derived exosomes and are easily isolated by using a magnet.[103] A comparative study on

isolation of tumor derived exosomes using iron oxide nano-particles, octahedral iron oxide nanocubes and nickel nano-wires revealed larger yield and higher purity of the isolated exosomes via nickel nanowires.

3. Exosome characterization techniques

Post-exosome isolation through different methods discussed in the prior sections, it is necessary to characterize the isolated exosomes for effective separation into subpopulations. There are various techniques of exosome characterization based on their biophysical or biological characteristics which have been developed in the past few decades (Fig. 5). These characterization techniques are useful for validating the upstream exosome isolation methods and categorizing exosome subpopulations for downstream analysis (Table 2).

3.1. Enzyme linked immunosorbent assay

Over the past few years, enzyme linked immunosorbent essay (ELISA) has been widely used for the characterization of exosomes via surface protein expression.[104–109] ELISA is a semi-quantitative protein detection methodology based on antigen–antibody specific binding. As a conventional method in immunology, it can be performed in multiple formats: sandwich method, indirect method, and competition method. For ELISA-based characterization, exosomes are usually immobilized on a microwell plate directly. After blocking the plates
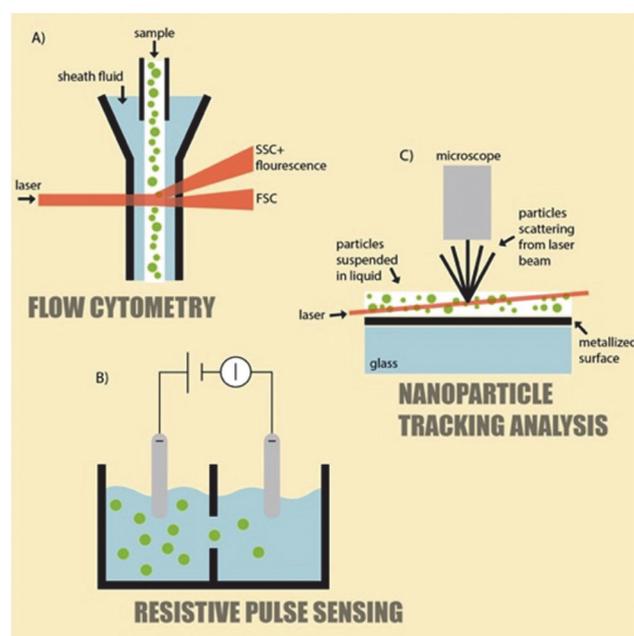
Fig. 5 Exosome characterization techniques. (A) Demonstrates the principle of flow cytometry. (B) Represents a schematic of tunable resistive pulse sensing. (C) Summarizes the principle of nanoparticle tracking analysis. Adapted from ref. 115 with permission from John Wiley and Sons, Copyright 2015.

Table 2 Summary of different exosome characterization techniques

Technique	Working principle	Biophysical/biochemical properties	Benefits	Disadvantages
Enzyme linked immunosorbent essay (ELISA)	Semi-quantitative protein detection methodology based on antigen–antibody specific binding	• Biochemical protein analysis • Monoplex detection using enzymatic labels (e.g. horseradish peroxidase or alkaline phosphatase)	• Rapid analysis • Cost-effective • High detection specificity	• Liable to biological noises such as nonspecific binding or adsorption of biomolecules
Western blotting	Detection of target proteins by specific antibodies through electrophoretic separation of complexes	• Biochemical protein analysis • Monoplex detection using enzymatic labels • Multiplex detection using chemiluminescent and/or fluorescent labels	• Workflow can be automated • High detection sensitivity and specificity	• Prolonged workflow and less amenable for high throughput adaptation
Flow cytometry	Quantification based on fluorescence and light scattering by individual exosome nanovesicles that are present in suspension	• Biophysical detection range of around 200–500 nm-sized particles • Biochemical protein analysis • Multiplex detection using fluorescent labels	• Rapid analysis • Capable of single-exosome analysis • High detection sensitivity and specificity	• Instrument-dependent variations among different laboratories • Unable to characterize smaller (<200 nm) nanovesicles
Nanoparticle tracking analysis (NTA)	Detection of nanovesicles moving in Brownian movement by a laser beam	• Biophysical detection range of around 50–1000 nm-sized particles • Biochemical protein analysis • Multiplex detection using fluorescent labels	• High detection sensitivity • Suitable for large number of samples	• Lengthy procedures involved in data acquisition and analysis
Tunable resistive pulse sensing (TRPS)	Detection of nano- or micro-sized particles by a decrease in the ionic current as measured across a tunable porous polyurethane membrane	• Biophysical detection range of around 70–10 000 nm-sized particles	• Accurate quantification and size characterization	• Unable to provide biochemical information
Laser tweezers Raman spectroscopy (LTRS)	Analysis of cellular and subcellular objects individually by Raman scattering via a tightly focused laser beam which traps and holds particles at the laser's focal point	• Biophysical detection range of around 20–80 000 nm-sized particles • Possible biochemical protein analysis using Raman spectral signatures	• Label-free analysis • Minimally disruptive method for analysis of native exosome state	• Provides population averaged information
Dynamic light scattering (DLS)	Determination of the differential size distribution of particles by illuminating with a laser beam for all particles present in the beam to scatter light.	• Biophysical detection range of around 100–10 000 nm-sized particles	• Small sample volumes required • Wide size and concentration range	• Requires careful data interpretation • Data interpretation requires shape and size distribution to be known
Atomic force microscopy (AFM)	Detection and recording of interactions between a probing tip and the sample surface	• Biophysical visualization range of around 1–8000 nm-sized particles	• Provides imaging of exosomes • Analysis of quantity, morphology, and biomechanics of exosomes	• Liable to measurement variations due to changes in temperature, AFM tip state, varying scan speed and force between tip and sample
Cryogenic electron microscopy (Cryo-EM)	Flash-freezing extracellular vesicles and then bombarding them with electrons to produce microscope images	• Biophysical visualization range of 30–450 nm-sized particles	• Maintains native hydrated exosome state • Provides high-resolution imaging of exosomes	• Requires extensive sample preparation • Bulky instrumentation • Costly set-up
Surface plasmon resonance (SPR) imaging	Real-time label-free monitoring of sample with variations in the molecular mass adsorbed on top of a gold layer	• Biophysical detection limit of <300 nm-sized particles • Biochemical protein analysis using immunoaffinity binding to gold surface	• Real-time analysis • Label free analysis • High detection specificity	• Difficult discrimination between specific and non-specific interactions

with a blocking agent, a recognition antibody (*e.g.*, anti-CD9) is added to the wells for binding to specific antigens (*e.g.*, CD9) that are presented on the exosome surface. Finally, a horseradish peroxidase-linked detection antibody is used for a sensitive (*via* an enzymatic signal amplification step) and specific readout. A colorimetric substrate (*e.g.*, 3,3′,5,5′-tetramethylbenzidine) is used for the assay read-out.[110,111] For examples, a sandwich ELISA has been demonstrated to capture and quantify exosomes in cell culture media and plasma samples by characterizing the housekeeping proteins CD63 and Rab-5b, as well as the tumor-associated marker caveolin-1.[104] One of the major drawbacks of ELISA-based exosome characterization is the high level of 'biological noise' (*i.e.* nonspecific binding or adsorption of biomolecules) in complex biological samples.

3.2. Western blotting

Western blotting, also known as immunoblotting, is based on the use of specific antibodies on gel electrophoresis-treated samples.[112] Western blotting is mostly used in extracellular vesicle research to characterize the presence of isolated exosomes *via* its specific surface proteins (CD9 and CD63). Western blotting is performed by first processing the exosome-containing sample with a lysis solution containing a protease inhibitor. The exosomes in the solution are then separated by sodium dodecyl sulphate polyacrylamide gel electrophoresis, which is then incubated with primary antibody and secondary antibodies after membrane transfer.

Western blotting is beneficial in providing information on the molecular weight of target exosome proteins in different subpopulations with low variability.[113] However, as compared to similarly immune-based ELISA, western blotting requires a lengthier workflow, more technical handling and expertise, and less amenable for high throughput adaptation.

3.3. Flow cytometry

Flow cytometry is a well-known technique for exosome characterization.[114,115] Flow cytometry is based on the recording of fluorescence and light scattering by individual exosome nanovesicles that are present in suspension. Initially, a single particle suspension is hydrodynamically focused with a sheath fluid to intersect with a laser.[115] Signals are obtained by a forward angle light scatter detector, a side-scatter detector, and multiple fluorescence emission detectors. Then, the signals are amplified and converted to digital format for analysis. However, conventional flow cytometry-based methods have several disadvantages.[115] The major concern is the platform-dependent variation which significantly varies among different laboratories. This variation is because different flow cytometers have different optical setups (*e.g.* varying laser wavelengths and powers) and different analytical sensitivities. Since exosomes have a lower refractive index than that of the conventional polystyrene beads used in the flow cytometer, the scattered light derived from similar-sized exosome nanovesicles is approximately ten-fold lower than that of the polystyrene beads.

A specialized type of flow cytometry is fluorescence-activated cell sorting (FACS) which allows the sorting of exosome nanovesicles based on fluorescent labeling.[116] This method involves a relatively more complex principle as compared to conventional flow cytometry. Using specific antibodies tagged with fluorescent dyes, the exosomes can be captured and sorted based on targeted surface protein expression. In recent years, FACS has been used for the characterization of exosome subpopulations.[115,117–120] For instance, Kim and colleagues developed a FACS-based technique for analysis of exosomes from murine lung-cancer cells.[121] In this methodology, the initial isolation of the exosomes was performed using CD9- or CD63-antibody-coated magnetic beads. After staining the sample with an *exo*-fluorescein isothiocyanate exosome staining solution, the analysis of exosomes was performed *via* FACS. The study reported an increased level of CD63-specific exosomes in LA-4 lung-cancer cells. In another study, Jasani *et al.* used a FACS technique to show the expression of the B-cell marker CD20 on B-cell exosomes.[122] First, the isolation of exosomes was conducted based on an immunomagnetic approach by anti-HLA-DP, DQ, and DR antibodies before subsequent FACS analysis was performed.

It is often suggested that 500 nm is the cut-off value for precise identification of nanoparticles using previous generations of flow cytometers.[111] Recently, a new generation of flow cytometers has been reported to enable the detection of nanovesicles smaller than 200 nm.[123] Nevertheless, the characterization of smaller nanovesicles by flow cytometry remains a challenge to be further improved upon. The high cost of flow cytometry is also prohibitive for exosome applications in resource-limited settings.

3.4. Nanoparticle tracking analysis

Nanoparticle tracking analysis (NTA) is the most widely used fluoresce-based tool for the characterization of exosome concentration and size due to its simplicity and ability to capture nanovesicles within the diameter range of 50–1000 nm.[124]

In NTA, a laser beam interacts with the exosome nanovesicles. The scattered light is captured by a charge-coupled device camera and then analysed by image processing software. The NTA software tracks the individual nanovesicles moving under Brownian motion and relates this movement to a particle size using the Stokes–Einstein equation. A comparison of NTA with flow cytometry using human placental exosomes suggests that NTA can measure the size of biological nanovesicles as small as ≈50 nm with a greater sensitivity.[125] NTA is also capable of characterizing a relatively larger amounts of nanovesicles as compared to electron microscopy and atomic force microscopy.[125]

Despite showing a reliability in fundamental research, NTA has substantial limitations in characterizing exosomes in clinical samples.[126] These limitations are due to the lengthy procedures involved in data acquisition. Specifically, flow cytometry can analyze 1000 particles in less than a second, whereas NTA will typically take around 10 min. Long analysis time also causes bleaching of the fluorescent dye (*i.e.* exosomes are

stained with common fluorescent dyes, such as green fluorescent protein or antibodies that are conjugated with fluorescein isothiocyanate), whereas flow cytometry is not limited to photobleaching as the readout is obtained in the shorter short time (≈1 s) before photobleaching occurs. Additionally, this tool cannot analyze the biochemical composition of distinct exosome subpopulations.

3.5. Tunable resistive pulse sensing

The commercial *qNano* system is based on the tunable resistive pulse sensing (TRPS) principle and developed for the quantitative characterization of nanosized particles.[127] This instrument uses tunable porous polyurethane membrane to detect the passage of nano- or micro-sized particles by a decrease in the ionic current as measured across the pores. The flexible nature of the pore membrane allows for the real-time optimization of the pore size. Many research groups have used TRPS to obtain measurements for exosome concentrations and also reported the use of TRPS for characterization of breast cancer-derived exosomes prior to quantifying them with surface plasmon resonance and electrochemical readouts.[128]

The *qNano* has shown great promise as a reliable tool for accurate exosome quantification and characterization. The TRPS technique provides a quantitative analysis of nanovesicles in the size range from 70 nm to 10 μm and performs real-time monitoring of ionic current flow across the pore to enable the detection of individual nanovesicles in mixed suspensions. However, TRPS also does not provide any biochemical information about the exosomes.

3.6. Laser tweezers Raman spectroscopy

Raman spectroscopy is a well-established, non-destructive and a non-contact method for chemical makeup analysis of a variety of samples.[11,129,130] Among the various forms of Raman spectroscopy, laser tweezers Raman spectroscopy (LTRS) holds great potential for characterizing exosomes. LTRS is a biophotonic tool which a tightly focused laser beam traps and holds small particles at the focal point of the beam. A confocal detection setup collects only Raman scattering from a precise focal volume, allowing cellular and sub-cellular objects to be studied/identified individually. This method has been used to study individual cancerous and non-cancerous cells,[131] activation response of individual immune cells,[132] as well as smaller nanoscale objects such as lipid droplets in milk, latex beads, and subcellular organelles (Fig. 6a).[133] However, LTRS could be challenged by precise classification of individual exosome subpopulations as it was found that clusters of exosomes trapped simultaneously in the laser focus eventually resulted in population averaged information without the ability to highlight the chemical composition differences within the exosome clusters.[134]

3.7. Dynamic light scattering

Dynamic light scattering (DLS), also known as photon correlation spectroscopy or quasi elastic light scattering, determines the differential size distribution of particles ranging in dia-

meter between sub-nm to several μm.[135] Similar to NTA, DLS also depends on the tracking of particles *via* Brownian motion. DLS is often used as a simple technique to measure the size distributions of extracellular vesicles to validate the sampling of exosome subpopulations.[136–138] The size distribution of these extracellular vesicles is obtained by measuring the intensity fluctuations of the scattered light, followed by applying a mathematical model derived from Brownian motion and light scattering theory. However, absolute quantification of extracellular vesicles cannot be performed with DLS because the mean signal amplitude depends on the diameter, concentration, and refractive index of the extracellular vesicles.[139] Using DLS, accurate size distributions are expected for monodisperse samples (samples containing extracellular vesicles of one particular size). However, size distributions of polydisperse samples (such as extracellular vesicles in human plasma) are less accurate and require foreknowledge of the sample to apply the most suitable mathematical model.[135,140] In general, DLS requires careful data interpretation and may be a useful method, provided that the shape of the size distribution is known.[138]

3.8. Atomic force microscopy

Atomic force microscopy (AFM) is a unique and reliable technique which gives better results as compared to optical and electron diffraction techniques for characterizing exosomes.[139] AFM has been used as a nanoscale tool to characterize the abundance, morphology, biomechanics, and biomolecular make-up of exosomes. Several studies have reported the effective use of AFM to characterize extracellular vesicles derived from blood, saliva (Fig. 6b),[141] and synovial fluid.[142]

AFM has increased the understanding of exosomes at the single- and sub-vesicular levels, and has provided useful information regarding the structural, biophysical, and biomolecular characteristics of a variety of sub-cellular structures. AFM can be used to quantify and simultaneously probe the structure, biomechanics, and biomolecular content of exosomes within heterogeneous populations.[143] An important feature of AFM is its ability to measure samples in native conditions, with minimal sample preparation and without any destructive mode of operation.[144,145] A major drawback of AFM is that measurement accuracy are susceptible to various factors like temperature, state of the AFM tip, force between probe and sample, or varying scan speed.[145]

3.9. Cryogenic electron microscopy

Electron microscopy is a standard method for characterizing extracellular vesicles. In the studies of many biological samples, cryogenic electron microscopy (cryo-EM) is commonly used.[146–148] The characteristic feature of isolated exosomes examined by transmission electron microscopy was observed to be a cup-shaped structure; however, frozen exosomes examined by cryo-EM showed the exosomes to be round in shape.[149] It was revealed that cryo-EM can preserve the true shapes of extracellular vesicles as the sample preparation in cryo-EM is free from dehydration and fixation. Because the
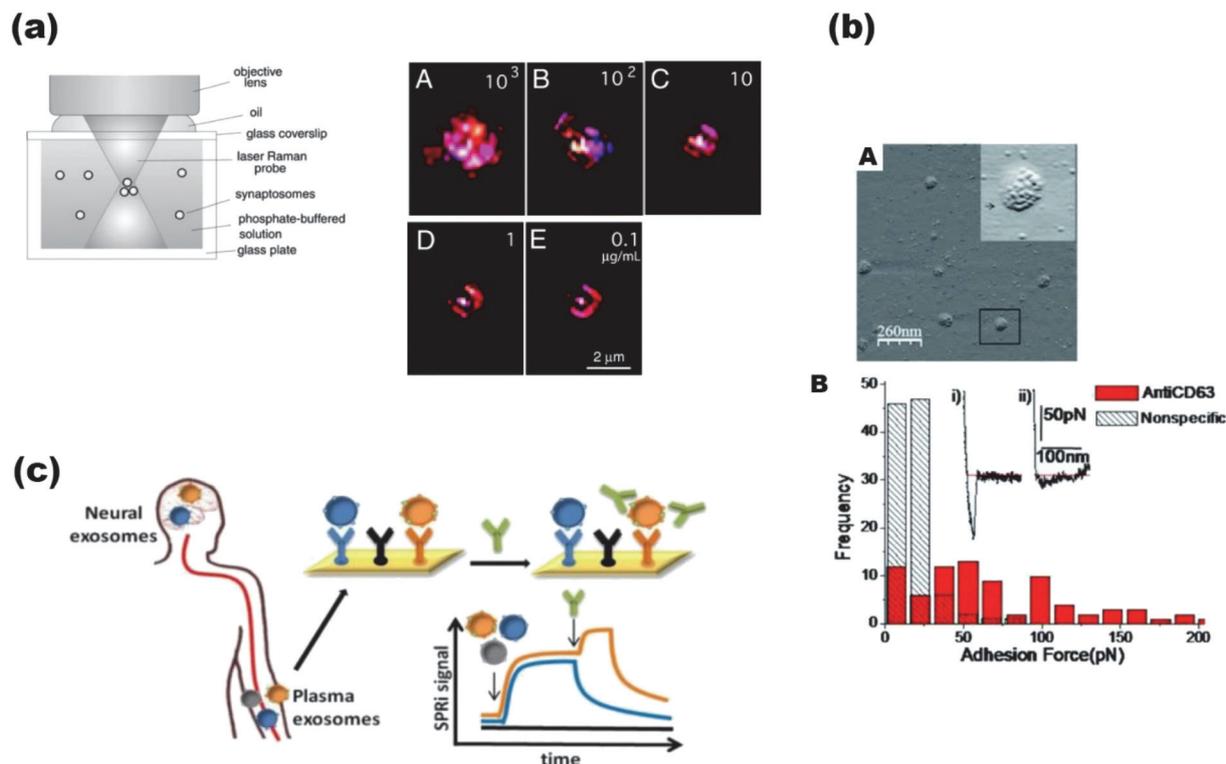
Fig. 6 (a) Optical set up for laser trapping of subcellular vesicles for Raman spectroscopy. Imaging of reflected light from different quantities – (A) 10^3, (B) 10^2, (C) 10, (D) 1, and (E) 0.1 – of aggregated and single subcellular vesicles during laser-trapping. Adapted from ref. 133 with permission from Royal Society of Chemistry, Copyright 2002. (b) Atomic force microscopy (AFM) imaging of exosomes with CD63 surface expression. (A) Image of 5–8 nm antibody-functionalized gold beads bound specifically to exosomes, inset shows a single exosome with surface-bound gold beads. (B) Distribution of rupture events by interaction forces between (i) antiCD63-coated or (ii) non-specific antibody-functionalized AFM tips and the exosome surface. Adapted from ref. 141 with permission from American Chemical Society, Copyright 2010. (c) Surface plasmon resonance imaging that uses antibodies against CD81 and GM1 for characterization of multiple exosome subpopulations in blood. Adapted from ref. 151 with permission from American Chemical Society, Copyright 2018.

samples are exposed to liquid nitrogen, the extracellular vesicles remain intact without ultrastructural changes or redistribution of elements. Cryo-EM is considered an ideal method for characterizing and visualizing nanovesicles without dehydration artifacts.

3.10. Surface plasmon resonance imaging

Surface plasmon resonance (SPR) imaging is a surface-based technique that allows real-time and label-free monitoring of sample *via* variations in the molecular mass adsorbed on top of a plasmonic layer. SPR is a promising approach to characterize exosome subpopulations with high detection specificity and sensitivity.[150]

Recently, Morasso and co-workers demonstrated a SPR imaging method to characterize a subpopulation of brain-derived exosomes within the bulk exosome population isolated from blood (Fig. 6c).[151] The bulk exosome population was initially pre-purified by size exclusion. Then an array of Abs was then used to separate the subpopulations of vesicles of different neural origin on distinct positions of the chip surface. The capture surface was functionalized to create self-assembled monolayer to target markers of neuronal and glial exosomes.

Subsequently, the amount of CD81 and GM1 markers on each exosome subpopulation was quantified using secondary antibodies binding to surface-immobilized exosomes.

As SPR is a mass sensitive technique, the sensitivity for high molecular weight molecules is good but the binding of low molecular weight compounds (*i.e.* smaller nanovesicles) will be more challenging to detect. Moreover, the sensor area is limited and has a limited capacity for large-scale target binding and characterization; this could be resolved by increasing the sensor surface area or performing several replicate runs.[152]

4. Existing challenges in separation of distinct exosome subpopulations

Evidently, precise separation of distinct exosome subpopulations remains cumbersome due to several technical as well as biological challenges associated with the limitations of existing isolation and characterization approaches.[153] Technical challenges include variation in preanalytical steps and lack of accurate separation approaches to sort distinct exosome subpopulation based on both biophysical and bio-

chemical attributes. Biological challenges include heterogeneous sample variation, specific separation of disease-associated exosomes from a background of normal exosomes, and the lack of integrated exosome cargo analysis to aid distinct exosome subpopulation sorting.

4.1. Technical challenges

It has been reported that variability in the different preanalytical steps; like sample collection, storage, use of anticoagulants and sample processing time that are involved in exosome isolation and characterization will affect the analysis outcomes. In this regard, the International Society for Extracellular Vesicles has started providing recommendations for a standardized and evidence-based workflow for extracellular vesicle analysis.[146] One common challenge involved in the sample collection procedure is the presence of impurities from activated platelet-derived vesicles due to the physical forces associated with the blood draw. Therefore, standardization of sampling sites, the use of right-sized needles, and good blood drawing technique are suggested to avoid the associated shear stress.[153,154]

Another recommendation is to avoid the use of heparin-based anticoagulants in the sample collection tube. This is because heparin can compete for biochemical binding, thereby resulting in inaccurate/biased immune-based exosome separation approaches.[155] Heparin has also been reported to inhibit the uptake of EV by recipient cells.[156] Therefore, as alternative choices for anticoagulants, ethylenediaminetetraacetic acid (EDTA), sodium fluoride, or sodium citrate in combination with or without different additives such as dextrose have been commonly used in collection tubes. Among these, citrate is generally preferred because EDTA was also found to interfere with downstream biochemical analysis.[157]

The discrepancy in exosome separation outcomes due to inappropriate storage conditions (e.g. freezing) is another hurdle to overcome. For large number of sample analyses, samples are generally collected from distant locations and freeze-stored prior to the analysis.[158,159] As this may affect exosome separation in samples, it is recommended to use freshly collected samples whenever possible.

The lack of consistent and specific methods to isolate and detect an enriched subpopulation of nano-sized exosomes (e.g. tumor-derived exosomes) among other normal exosomes makes the exosome subpopulation separation process a challenging task. Thus, there is an urgent need for an integrated approach for specific separation of distinct exosome subpopulations based on both biophysical and biochemical attributes.

Over the past years, conventional exosome isolation methods have attempted to sort exosomes based on either biophysical (e.g. size) or biochemical (e.g. surface protein expression) characteristics. For example, differential ultracentrifugation is one of the most widely used methods for size-based exosome isolation, but it does not consider the immune-profiles of various exosome subpopulations. Indeed, as discussed in the previous sections, all isolation methods have their unique benefits and shortfalls. For instance, ultra-

centrifugation frequently suffers from the loss of exosomes and co-pelleted impurities during the isolation process. On the other hand, immunoaffinity-based isolation methods provide high immune-selectivity but are limited by lower isolated exosome yields. To utilize the benefits of the various isolation methods for accurate separation of distinct exosome subpopulations, it is proposed to combine size-based and immunoaffinity-based methods into an integrated approach.

The combination of ultrafiltration and ultracentrifugation techniques has been shown to generate clinical grade exosomes. In a similar manner, ultracentrifugation can be first used to concentrate large volumes of samples and extensively process bulk exosomes before incubating with antibodies/aptamers-coated superparamagnetic nanoparticles and further separate exosomes by immunoaffinity. The use of microfluidics can also offer a miniaturized platform to integrate feasible approaches such as ultrafiltration and magnetic isolation. It is envisioned that multiplex exosome surface proteins could be utilized simultaneously to enable effective separation of distinct subpopulations.[160]

4.2. Biological challenges

Many genetic, physiological, and environmental factors that are associated with sample heterogeneity can affect exosome separation. Across different individuals, disease-specific exosomes can be present in different subpopulations than normal state due to varying individual factors such as age, gender, body mass index, and immunity.[153] Therefore, choosing an ideal control which normalizes for individual exosome subpopulation variations across heterogeneous samples is a significant challenge (i.e. a control derived from young individuals cannot reliably be used to analyze exosomes that are derived from elderly people). Thus, more systemic studies are needed to study the effects of sample heterogeneity on the biogenesis, functionality, and quantity of exosomes. Importantly, there is an urgent need to establish a predesigned sample control bank, which contains controls from all possible variants of the target population; such as different ages, races, sexes, physiological conditions, etc. Although recent progress has improved the separation efficiency of exosomes from other extracellular vesicles, there are only few reported strategies that described the differentiation of disease-specific exosomes from the background of normal exosomes.[161]

It is now widely acknowledged that exosome cargo, which is encapsulated in the protective layer of the exosome membrane, is a promising source of biomarkers for disease diagnosis and prognosis. This is because the cargo is protected from many harsh conditions inside the encapsulated protective environment of the exosomes (e.g., exosomal miRNA is protected from ribonuclease-mediated degradation). In addition to exosome isolation and characterization based on external biophysical and biochemical traits, it would be useful to utilize the internal molecular information within the exosome cargo for distinct exosome subpopulation sorting.[162] While this would incur multiple additional steps in the analysis of released molecular cargo from the isolated exosomes, such deeper analysis into distinct

exosome subpopulations could yet yield valuable insights into the many unanswered fundamental questions concerning the functionalities of exosomes and their contents.[8] For instance, it is still unclear whether the transport and uptake of exosomes by distant recipient cells are due to phagocytosis[163] or uptake by selective receptors of distant recipient cells.[164]

5. Conclusions and future perspectives

It is our belief that both isolation and characterization approaches will enable reliable separation of exosomes into distinct subpopulations based on biophysical and biochemical traits. As reviewed herein, the existing and emerging vast arsenal of isolation and characterization approaches have enabled the modern separation of exosomes for research and clinical studies. In line with the highlighted technical and biological challenges, it is highly anticipated that these exosome separation approaches will further progress towards accurate sorting of distinct exosome subpopulations to overcome the obstacle of exosome heterogeneity.

It is highly anticipated that the ability to reproducibly isolate and characterize a heterogeneous exosome population into well-defined subpopulations will pave the way towards novel mechanism insights of exosome-based cellular communication. To date, the "one-size-fits-all" exosome separation strategy based on using a singular isolation/characterization step for bulk exosomes has uncovered fundamental insights into the role of exosomes in the progression of several diseases. Crucially, this has also taught us that disease-associated exosomes, as similar to circulating tumor cells or mutated nucleic acid sequences, require differentiative sorting from their normal/wildtype counterparts.

Moving forwards, we predict that exosome separation will evolve towards using initial biophysical isolation for nanovesicle enrichment, followed by more stringent biochemical isolation to inform biological/clinical information. Along this workflow, accurate characterization techniques will ensure the quality of isolation outcomes. The use of a combination of different isolation and characterization approaches in our existing toolbox can currently enable the separation of distinct exosome subpopulations, whist the cutting-edge advancements in microfluidics and nanomaterials can further improve the efficiency of the entire process.

Conflicts of interest

There are no conflicts of interest to declare.

Acknowledgements

References

1 M. P. Zaborowski, L. Balaj, X. O. Breakefield and C. P. Lai, *BioScience*, 2015, **65**, 783–797.

2 J. De Toro, L. Herschlik, C. Waldner and C. Mongini, *Front. Immunol.*, 2015, **6**, 203.

3 A. Möller and R. J. Lobb, *Nat. Rev. Cancer*, 2020, **20**, 697–709.

4 Y. Cheng, J. S. Schorey, P. P. Singh and V. L. Smith, *EMBO Rep.*, 2014, **16**, 24–43.

5 A. Shimoda, S. Nishiumi, N. Murata-Kamiya, S.-A. Mukai, S.-I. Sawada, T. Azuma, M. Hatakeyama and K. Akiyoshi, *Sci. Rep.*, 2016, **6**, 18346.

6 K. M. Koo, P. N. Mainwaring, S. A. Tomlins and M. Trau, *Nat. Rev. Urol.*, 2019, **16**, 302–317.

7 E. Willms, C. Cabañas, I. Mäger, M. J. A. Wood and P. Vader, *Front. Immunol.*, 2018, **9**, 738.

8 E. Willms, H. J. Johansson, I. Mäger, Y. Lee, K. E. M. Blomberg, M. Sadik, A. Alaarg, C. I. E. Smith, J. Lehtiö, S. El Andaloussi, M. J. A. Wood and P. Vader, *Sci. Rep.*, 2016, **6**, 22519.

9 J. Wang, K. M. Koo, Y. Wang and M. Trau, *Adv. Sci.*, 2019, **6**, 1900730.

10 B. Mateescu, E. J. K. Kowal, B. W. M. van Balkom, S. Bartel, S. N. Bhattacharyya, E. I. Buzás, A. H. Buck, P. de Candia, F. W. N. Chow, S. Das, T. A. P. Driedonks, L. Fernández-Messina, F. Haderk, A. F. Hill, J. C. Jones, K. R. Van Keuren-Jensen, C. P. Lai, C. Lässer, I. d. Liegro, T. R. Lunavat, M. J. Lorenowicz, S. L. N. Maas, I. Mäger, M. Mittelbrunn, S. Momma, K. Mukherjee, M. Nawaz, D. M. Pegtel, M. W. Pfaffl, R. M. Schiffelers, H. Tahara, C. Théry, J. P. Tosar, M. H. M. Wauben, K. W. Witwer and E. N. M. Nolte-'t Hoen, *J. Extracell. Vesicles*, 2017, **6**, 1286095.

11 Z. J. Smith, C. Lee, T. Rojalin, R. P. Carney, S. Hazari, A. Knudson, K. Lam, H. Saari, E. L. Ibañez, T. Viitala, T. Laaksonen, M. Yliperttula and S. Wachsmann-Hogiu, *J. Extracell. Vesicles*, 2015, **4**, 28533.

12 S. Matsumura, T. Minamisawa, K. Suga, H. Kishita, T. Akagi, Y. Ichiki, Y. Ichikawa and K. Shiba, *J. Extracell. Vesicles*, 2019, **8**, 1579541.

13 Z. Chen, Y. Yang, H. Yamaguchi, M. C. Hung and J. Kameoka, *Biomicrofluidics*, 2020, **14**, 034113.

14 M. Tkach, J. Kowal and C. Théry, *Philos. Trans. R. Soc. London, Ser. B*, 2018, **373**, 20160479.

15 M. S. Kim, M. J. Haney, Y. Zhao, V. Mahajan, I. Deygen, N. L. Klyachko, E. Inskoe, A. Piroyan, M. Sokolsky, O. Okolie, S. D. Hingtgen, A. V. Kabanov and E. V. Batrakova, *Nanomedicine*, 2016, **12**, 655–664.

16 S. Kamerkar, V. S. LeBleu, H. Sugimoto, S. Yang, C. F. Ruivo, S. A. Melo, J. J. Lee and R. Kalluri, *Nature*, 2017, **546**, 498–503.

17 P. Li, M. Kaslan, S. H. Lee, J. Yao and Z. Gao, *Theranostics*, 2017, **7**, 789–804.

18 X. Li, A. L. Corbett, E. Taatizadeh, N. Tasnim, J. P. Little, C. Garnis, M. Daugaard, E. Guns, M. Hoorfar and I. T. S. Li, *APL Bioeng.*, 2019, **3**, 011503.

19 M. Logozzi, D. Mizzoni, R. Di Raimo and S. Fais, *Cancer*, 2020, **12**, 2566.

20 J. Howard, C. Wyse, D. Argyle, C. Quinn, P. Kelly and A. McCann, *Biochim. Biophys. Acta, Rev. Cancer*, 2020, **1874**, 188431.

21 X. Zhang, X. Yuan, H. Shi, L. Wu, H. Qian and W. Xu, *J. Hematol. Oncol.*, 2015, **8**, 83.

22 S. Principe, A. B. Hui, J. Bruce, A. Sinha, F. F. Liu and T. Kislinger, *Proteomics*, 2013, **13**, 1608–1623.

23 D. Yang, W. Zhang, H. Zhang, F. Zhang, L. Chen, L. Ma, L. M. Larcher, S. Chen, N. Liu, Q. Zhao, P. H. L. Tran, C. Chen, R. N. Veedu and T. Wang, *Theranostics*, 2020, **10**, 3684–3707.

24 R. Hou, Y. Li, Z. Sui, H. Yuan, K. Yang, Z. Liang, L. Zhang and Y. Zhang, *Anal. Bioanal. Chem.*, 2019, **411**, 5351–5361.

25 L. M. Doyle and M. Z. Wang, *Cells*, 2019, **8**, 727.

26 C. Théry, S. Amigorena, G. Raposo and A. Clayton, *Curr. Protoc. Cell Biol.*, 2006, **30**, 3.22.1–3.22.29.

27 O. Rechavi, Y. Erlich, H. Amram, L. Flomenblit, F. V. Karginov, I. Goldstein, G. J. Hannon and Y. Kloog, *Genes Dev.*, 2009, **23**, 1971–1979.

28 E. Zeringer, T. Barta, M. Li and A. V. Vlassov, *Cold Spring Harb. Protoc.*, 2015, **2015**, 319–323.

29 S. Gupta, S. Rawat, V. Arora, S. K. Kottarath, A. K. Dinda, P. K. Vaishnav, B. Nayak and S. Mohanty, *Stem Cell Res. Ther.*, 2018, **9**, 180.

30 J. Kowal, G. Arras, M. Colombo, M. Jouve, J. P. Morath, B. Primdal-Bengtson, F. Dingli, D. Loew, M. Tkach and C. Thery, *Proc. Natl. Acad. Sci. U. S. A.*, 2016, **113**, E968–E977.

31 S. Kreimer and A. R. Ivanov, *Methods Mol. Biol.*, 2017, **1660**, 295–302.

32 J. Z. Nordin, Y. Lee, P. Vader, I. Mager, H. J. Johansson, W. Heusermann, O. P. Wiklander, M. Hallbrink, Y. Seow, J. J. Bultema, J. Gilthorpe, T. Davies, P. J. Fairchild, S. Gabrielsson, N. C. Meisner-Kober, J. Lehtio, C. I. Smith, M. J. Wood and S. El Andaloussi, *Nanomedicine*, 2015, **11**, 879–883.

33 K. Boriachek, M. N. Islam, A. Moller, C. Salomon, N.-T. Nguyen, M. S. A. Hossain, Y. Yamauchi and M. J. A. Shiddiky, *Small*, 2018, **14**, 201702153.

34 F. Liu, O. Vermesh, V. Mani, T. J. Ge, S. J. Madsen, A. Sabour, E. C. Hsu, G. Gowrishankar, M. Kanada, J. V. Jokerst, R. G. Sierra, E. Chang, K. Lau, K. Sridhar, A. Bermudez, S. J. Pitteri, T. Stoyanova, R. Sinclair, V. S. Nair, S. S. Gambhir and U. Demirci, *ACS Nano*, 2017, **11**, 10712–10723.

35 A. N. Boing, E. van der Pol, A. E. Grootemaat, F. A. Coumans, A. Sturk and R. Nieuwland, *J. Extracell. Vesicles*, 2014, **3**, 23430.

36 I. Lozano-Ramos, I. Bancu, A. Oliveira-Tercero, M. P. Armengol, A. Menezes-Neto, H. A. Del Portillo, R. Lauzurica-Valdemoros and F. E. Borras, *J. Extracell. Vesicles*, 2015, **4**, 27369.

37 R. Vogel, F. A. Coumans, R. G. Maltesen, A. N. Boing, K. E. Bonnington, M. L. Broekman, M. F. Broom, E. I. Buzas, G. Christiansen, N. Hajji, S. R. Kristensen, M. J. Kuehn, S. M. Lund, S. L. Maas, R. Nieuwland, X. Osteikoetxea, R. Schnoor, B. J. Scicluna, M. Shambrook, J. de Vrij, S. I. Mann, A. F. Hill and S. Pedersen, *J. Extracell. Vesicles*, 2016, **5**, 31242.

38 K. E. Petersen, F. Shiri, T. White, G. T. Bardi, H. Sant, B. K. Gale and J. L. Hood, *Anal. Chem.*, 2018, **90**, 12783–12790.

39 K. Agarwal, M. Saji, S. M. Lazaroff, A. F. Palmer, M. D. Ringel and M. E. Paulaitis, *Langmuir*, 2015, **31**, 5440–5448.

40 K. E. Petersen, E. Manangon, J. L. Hood, S. A. Wickline, D. P. Fernandez, W. P. Johnson and B. K. Gale, *Anal. Biochem.*, 2014, **406**, 7855–7866.

41 C. Chen, J. Skog, C. H. Hsu, R. T. Lessard, L. Balaj, T. Wurdinger, B. S. Carter, X. O. Breakefield, M. Toner and D. Irimia, *Lab Chip*, 2010, **10**, 505–511.

42 C. E. Yoo, G. Kim, M. Kim, D. Park, H. J. Kang, M. Lee and N. Huh, *Anal. Biochem.*, 2012, **431**, 96–98.

43 Z. Zhao, Y. Yang, Y. Zeng and M. He, *Lab Chip*, 2016, **16**, 489–496.

44 K. M. Koo, E. J. H. Wee, Y. Wang and M. Trau, *Lab Chip*, 2017, **17**, 3200–3220.

45 D. K. Kang, X. Gong, S. Cho, J. Y. Kim, J. B. Edel, S. I. Chang, J. Choo and A. J. deMello, *Anal. Chem.*, 2015, **87**, 10770–10778.

46 M. T. Guo, A. Rotem, J. A. Heyman and D. A. Weitz, *Lab Chip*, 2012, **12**, 2146–2155.

47 J. Shuga, Y. Zeng, R. Novak, Q. Lan, X. Tang, N. Rothman, R. Vermeulen, L. Li, A. Hubbard, L. Zhang, R. A. Mathies and M. T. Smith, *Nucleic Acids Res.*, 2013, **41**, e159.

48 Y. Zeng, R. Novak, J. Shuga, M. T. Smith and R. A. Mathies, *Anal. Chem.*, 2010, **82**, 3183–3190.

49 D. Witters, K. Knez, F. Ceyssens, R. Puers and J. Lammertyn, *Lab Chip*, 2013, **13**, 2047–2054.

50 A. Liga, A. D. Vliegenthart, W. Oosthuyzen, J. W. Dear and M. Kersaudy-Kerhoas, *Lab Chip*, 2015, **15**, 2388–2394.

51 C. Chen, J. Skog, C.-H. Hsu, R. T. Lessard, L. Balaj, T. Wurdinger, B. S. Carter, X. O. Breakefield, M. Toner and D. Irimia, *Lab Chip*, 2010, **10**, 505–511.

52 C. L. Hisey, K. D. P. Dorayappan, D. E. Cohn, K. Selvendiran and D. J. Hansford, *Lab Chip*, 2018, **18**, 3144–3153.

53 K. D. P. Dorayappan, M. L. Gardner, C. L. Hisey, R. A. Zingarelli, B. Q. Smith, M. D. S. Lightfoot, R. Gogna, M. M. Flannery, J. Hays, D. J. Hansford, M. A. Freitas, L. Yu, D. E. Cohn and K. Selvendiran, *Cancer Res.*, 2019, **79**, 3503–3513.

54 D. C. Duffy, J. C. McDonald, O. J. Schueller and G. M. Whitesides, *Anal. Chem.*, 1998, **70**, 4974–4984.

55 S. Bakshi, K. Pandey, S. Bose, P. D. Gunjan and R. Nayak, *J. Colloid Interface Sci.*, 2019, **552**, 34–42.

56 B. A. Ashcroft, J. de Sonneville, Y. Yuana, S. Osanto, R. Bertina, M. E. Kuil and T. H. Oosterkamp, *Biomed. Microdevices*, 2012, **14**, 641–649.

57 P. Zhang, M. He and Y. Zeng, *Lab Chip*, 2016, **16**, 3033–3042.

58 W. Hu, G. He, H. Zhang, X. Wu, J. Li, Z. Zhao, Y. Qiao, Z. Lu, Y. Liu and C. M. Li, *Anal. Chem.*, 2014, **86**, 4488–4493.

59 H. J. Yoon, T. H. Kim, Z. Zhang, E. Azizi, T. M. Pham, C. Paoletti, J. Lin, N. Ramnath, M. S. Wicha, D. F. Hayes, D. M. Simeone and S. Nagrath, *Nat. Nanotechnol.*, 2013, **8**, 735–741.

60 A. S. Azmi, B. Bao, F. H. Sarkar and M. Reviews, *Cancer Metastasis Rev.*, 2013, **32**, 623–642.

61 S. S. Kanwar, C. J. Dunlay, D. M. Simeone and S. Nagrath, *Lab Chip*, 2014, **14**, 1891–1900.

62 M. He, J. Crow, M. Roth, Y. Zeng and A. K. Godwin, *Lab Chip*, 2014, **14**, 3773–3780.

63 S. Fang, H. Tian, X. Li, D. Jin, X. Li, J. Kong, C. Yang, X. Yang, Y. Lu, Y. Luo, B. Lin, W. Liu and T. Liu, *PLoS One*, 2017, **12**, e0175050.

64 H. Im, K. Lee, R. Weissleder, H. Lee and C. M. Castro, *Lab Chip*, 2017, **17**, 2892–2898.

65 T. Laurell, F. Petersson and A. Nilsson, *Chem. Soc. Rev.*, 2007, **36**, 492–506.

66 P. Li, Z. Mao, Z. Peng, L. Zhou, Y. Chen, P. H. Huang, C. I. Truica, J. J. Drabick, W. S. El-Deiry, M. Dao, S. Suresh and T. J. Huang, *Proc. Natl. Acad. Sci. U. S. A.*, 2015, **112**, 4970–4975.

67 J. Dual and T. Schwarz, *Lab Chip*, 2012, **12**, 244–252.

68 J. Friend, *Rev. Mod. Phys.*, 2011, **83**, 647.

69 B. Watson, J. Friend and L. Yeo, *Sens. Actuators, A*, 2009, **152**, 219–233.

70 J. Dual and D. Moller, *Lab Chip*, 2012, **12**, 506–514.

71 K. Lee, H. Shao, R. Weissleder and H. Lee, *ACS Nano*, 2015, **9**, 2321–2327.

72 X. Ding, P. Li, S. C. Lin, Z. S. Stratton, N. Nama, F. Guo, D. Slotcavage, X. Mao, J. Shi, F. Costanzo and T. J. Huang, *Lab Chip*, 2013, **13**, 3626–3649.

73 G. Destgeer and H. J. Sung, *Lab Chip*, 2015, **15**, 2722–2738.

74 D. B. Go, M. Z. Atashbar, Z. Ramshani and H. C. Chang, *Anal. Methods*, 2017, **9**, 4112–4134.

75 J. C. Contreras-Naranjo, H. J. Wu and V. M. Ugaz, *Lab Chip*, 2017, **17**, 3558–3577.

76 R. T. Davies, J. Kim, S. C. Jang, E. J. Choi, Y. S. Gho and J. Park, *Lab Chip*, 2012, **12**, 5202–5210.

77 L. G. Liang, M. Q. Kong, S. Zhou, Y. F. Sheng, P. Wang, T. Yu, F. Inci, W. P. Kuo, L. J. Li, U. Demirci and S. Wang, *Sci. Rep.*, 2017, **7**, 46224.

78 H. K. Woo, V. Sunkara, J. Park, T. H. Kim, J. R. Han, C. J. Kim, H. I. Choi, Y. K. Kim and Y. K. Cho, *ACS Nano*, 2017, **11**, 1360–1370.

79 J. Dong, R. Y. Zhang, N. Sun, M. Smalley, Z. Wu, A. Zhou, S. J. Chou, Y. J. Jan, P. Yang, L. Bao, D. Qi, X. Tang, P. Tseng, Y. Hua, D. Xu, R. Kao, M. Meng, X. Zheng, Y. Liu, T. Vagner, X. Chai, D. Zhou, M. Li, S. H. Chiou, G. Zheng, D. Di Vizio, V. G. Agopian, E. Posadas, S. J. Jonas, S. P. Ju, P. S. Weiss, M. Zhao, H. R. Tseng and Y. Zhu, *ACS Appl. Mater. Interfaces*, 2019, **11**, 13973–13983.

80 J. Dong, R. Y. Zhang, N. Sun, J. Hu, M. D. Smalley, A. Zhou, Y. Hua, W. Rothermich, M. Chen, J. Chen, J. Ye, P.-C. Teng, D. Qi, J. A. Toretsky, J. S. Tomlinson, M. Li, P. S. Weiss, S. J. Jonas, N. Federman, L. Wu, M. Zhao, H.-R. Tseng and Y. Zhu, *Adv. Funct. Mater.*, 2020, 2003237.

81 N. Sun, Y.-T. Lee, R. Y. Zhang, R. Kao, P.-C. Teng, Y. Yang, P. Yang, J. J. Wang, M. Smalley, P.-J. Chen, M. Kim, S.-J. Chou, L. Bao, J. Wang, X. Zhang, D. Qi, J. Palomique, N. Nissen, S.-H. B. Han, S. Sadeghi, R. S. Finn, S. Saab, R. W. Busuttil, D. Markovic, D. Elashoff, H.-H. Yu, H. Li, A. P. Heaney, E. Posadas, S. You, J. D. Yang, R. Pei, V. G. Agopian, H.-R. Tseng and Y. Zhu, *Nat. Commun.*, 2020, **11**, 4489.

82 Z. Wang, H. J. Wu, D. Fine, J. Schmulen, Y. Hu, B. Godin, J. X. Zhang and X. Liu, *Lab Chip*, 2013, **13**, 2879–2882.

83 Y. Wang, H. Xu, J. Zhang and G. Li, *Sensors*, 2008, **8**, 2043–2081.

84 A. Chamorro-Garcia and A. Merkoci, *Nanobiomedicine*, 2016, **3**, 1849543516663574.

85 M. K. Masud, J. Na, M. Younus, M. S. A. Hossain, Y. Bando, M. J. A. Shiddiky and Y. Yamauchi, *Chem. Soc. Rev.*, 2019, **48**, 5717–5751.

86 K. Boriachek, M. K. Masud, C. Palma, H. P. Phan, Y. Yamauchi, M. S. A. Hossain, N.-T. Nguyen, C. Salomon and M. J. A. Shiddiky, *Anal. Chem.*, 2019, **91**, 3827–3834.

87 N. Xia and L. Zhang, *Materials*, 2014, **7**, 5366–5384.

88 S. Sharma, M. N. Javed, F. H. Pottoo, S. A. Rabbani, M. A. Barkat, M. Sarafroz and M. Amir, *Pharm. Nanotechnol.*, 2019, **7**, 220–233.

89 X. Huang, Y. Liu, B. Yung, Y. Xiong and X. Chen, *ACS Nano*, 2017, **11**, 5238–5292.

90 K. M. Koo, N. Soda and M. J. A. Shiddiky, *Curr. Opin. Electrochem.*, 2020, **25**, 100645.

91 J. D. Ryckman, M. Liscidini, J. E. Sipe and S. M. Weiss, *Nano Lett.*, 2011, **11**, 1857–1862.

92 M. Chang, Y. J. Chang, P. Y. Chao and Q. Yu, *PLoS One*, 2018, **13**, e0199438.

93 F. Wei, J. Yang and D. T. W. Wong, *Biosens. Bioelectron.*, 2013, **44**, 115–121.

94 K. Boriachek, M. N. Islam, V. Gopalan, A. K. Lam, N.-T. Nguyen and M. J. A. Shiddiky, *Analyst*, 2017, **142**, 2211–2219.

95 Y. Zhuo, P.-X. Yuan, R. Yuan, Y.-Q. Chai and C.-L. Hong, *Biomaterials*, 2009, **30**, 2284–2290.

96 S. Krishnan, V. Mani, D. Wasalathanthri, C. V. Kumar and J. F. Rusling, *Angew. Chem., Int. Ed.*, 2011, **50**, 1175–1178.

97 S. Bi, Y. Yan, X. Yang and S. Zhang, *Chemistry*, 2009, **15**, 4704–4709.

98 D.-X. Nie, G.-Y. Shi and Y.-Y. Yu, *Chin. J. Anal. Chem.*, 2016, **44**, 179–185.

99 H. Wei and E. Wang, *Chem. Soc. Rev.*, 2013, **42**, 6060–6093.

100 Z. Nemati, J. Um, M. R. Z. Kouhpanji, F. Zhou, T. Gage, D. Shore, K. Makielski, A. Donnelly and J. Alonso, *ACS Appl. Nano Mater.*, 2020, **3**, 2058–2069.

101 J. Lim, M. Choi, H. Lee, Y.-H. Kim, J.-Y. Han, E. S. Lee and Y. Cho, *J. Nanobiotechnol.*, 2019, **17**, 1.

102 J. Lim, M. Choi, H. Lee, J. Y. Han and Y. Cho, *Front. Chem.*, 2018, **6**, 664.

103 Z. Nemati, M. R. Zamani Kouhpanji, F. Zhou, R. Das, K. Makielski, J. Um, M. H. Phan, A. Muela, M. L. Fdez-Gubieda, R. R. Franklin, B. J. H. Stadler, J. F. Modiano and J. Alonso, *Nanomaterials*, 2020, **10**, 1662.

104 M. Logozzi, A. De Milito, L. Lugini, M. Borghi, L. Calabro, M. Spada, M. Perdicchio, M. L. Marino, C. Federici, E. Iessi, D. Brambilla, G. Venturi, F. Lozupone, M. Santinami, V. Huber, M. Maio, L. Rivoltini and S. Fais, *PLoS One*, 2009, **4**, e5219.

105 S. Khan, H. F. Bennit, D. Turay, M. Perez, S. Mirshahidi, Y. Yuan and N. R. Wall, *BMC Cancer*, 2014, **14**, 176.

106 Z. C. Hartman, J. Wei, O. K. Glass, H. Guo, G. Lei, X.-Y. Yang, T. Osada, A. Hobeika, A. Delcayre, J.-B. Le Pecq, M. A. Morse, T. M. Clay and H. K. Lyerly, *Vaccine*, 2011, **29**, 9361–9367.

107 H. G. Lamparski, A. Metha-Damani, J.-Y. Yao, S. Patel, D.-H. Hsu, C. Ruegg and J.-B. Le Pecq, *J. Immunol. Methods*, 2002, **270**, 211–226.

108 J. N. Higginbotham, M. D. Beckler, J. D. Gephart, J. L. Franklin, G. Bogatcheva, G.-J. Kremers, D. W. Piston, G. D. Ayers, R. E. McConnell, M. J. Tyska and R. J. Coffey, *Curr. Biol.*, 2011, **21**, 779–786.

109 J. Webber, R. Steadman, M. D. Mason, Z. Tabi and A. Clayton, *Cancer Res.*, 2010, **70**, 9621–9630.

110 B. K. Van Weemen and A. H. W. M. Schuurs, *FEBS Lett.*, 1971, **15**, 232–236.

111 E. Engvall and P. J. I. Perlmann, *Immunochemistry*, 1971, **8**, 871–874.

112 Z. Fan, J. Yu, J. Lin, Y. Liu and Y. J. A. Liao, *Analyst*, 2019, **144**, 5856–5865.

113 N. Zarovni, A. Corrado, P. Guazzi, D. Zocco, E. Lari, G. Radano, J. Muhhina, C. Fondelli, J. Gavrilova and A. J. M. Chiesi, *Methods*, 2015, **87**, 46–58.

114 S. Robert, P. Poncelet, R. Lacroix, L. Arnaud, L. Giraudo, A. Hauchard, J. Sampol and F. Dignat-George, *J. Thromb. Haemostasis*, 2009, **7**, 190–197.

115 U. Erdbrügger and J. Lannigan, *Cytometry, Part A*, 2016, **89**, 123–134.

116 H. K. Kim, K. S. Song, E. S. Lee, Y. J. Lee, Y. S. Park, K. R. Lee and S. N. Lee, *Blood Coagulation Fibrinolysis*, 2002, **13**, 393–397.

117 M. H. Julius, T. Masuda and L. A. Herzenberg, *Proc. Natl. Acad. Sci. U. S. A.*, 1972, **69**, 1934–1938.

118 M. P. Hunter, N. Ismail, X. Zhang, B. D. Aguda, E. J. Lee, L. Yu, T. Xiao, J. Schafer, M.-L. T. Lee, T. D. Schmittgen, S. P. Nana-Sinkam, D. Jarjoura and C. B. Marsh, *PLoS One*, 2008, **3**, e3694.

119 J. I. Zwicker, R. Lacroix, F. Dignat-George, B. C. Furie and B. Furie, *Methods Mol. Biol.*, 2012, **788**, 127–139.

120 M. Kesimer, M. Scull, B. Brighton, G. DeMaria, K. Burns, W. O'Neal, R. J. Pickles and J. K. Sheehan, *FASEB J.*, 2009, **23**, 1858–1868.

121 K.-T. Rim and S.-J. Kim, *J. Cancer Prev.*, 2016, **21**, 194–200.

122 A. Clayton, J. Court, H. Navabi, M. Adams, M. D. Mason, J. A. Hobot, G. R. Newman and B. Jasani, *J. Immunol. Methods*, 2001, **247**, 163–174.

123 R. Lacroix, S. Robert, P. Poncelet and F. Dignat-George, *Semin. Thromb. Hemostasis*, 2010, **36**, 807–818.

124 C. Y. Soo, Y. Song, Y. Zheng, E. C. Campbell, A. C. Riches, F. Gunn-Moore and S. J. Powis, *Immunology*, 2012, **136**, 192–197.

125 R. A. Dragovic, C. Gardiner, A. S. Brooks, D. S. Tannetta, D. J. Ferguson, P. Hole, B. Carr, C. W. Redman, A. L. Harris, P. J. Dobson, P. Harrison and I. L. Sargent, *Nanomedicine*, 2011, **7**, 780–788.

126 E. Van der Pol, A. N. Böing, E. L. Gool and R. Nieuwland, *J. Thromb. Haemostasis*, 2016, **14**, 48–56.

127 R. Vogel, G. Willmott, D. Kozak, G. S. Roberts, W. Anderson, L. Groenewegen, B. Glossop, A. Barnett, A. Turner and M. Trau, *Anal. Chem.*, 2011, **83**, 3499–3506.

128 A. A. I. Sina, R. Vaidyanathan, S. Dey, L. G. Carrascosa, M. J. A. Shiddiky and M. Trau, *Sci. Rep.*, 2016, **6**, 30460.

129 Y. Zeng, K. M. Koo, M. Trau, A.-G. Shen and J.-M. Hu, *Appl. Mater. Today*, 2019, **15**, 431–444.

130 S. Dey, M. Trau and K. M. Koo, *Nanomaterials*, 2020, **10**, 1145.

131 K. Chen, Y. Qin, F. Zheng, M. Sun and D. Shi, *Opt. Lett.*, 2006, **31**, 2015–2017.

132 J. W. Chan, D. S. Taylor, S. M. Lane, T. Zwerdling, J. Tuscano and T. Huser, *Anal. Chem.*, 2008, **80**, 2180–2187.

133 K. Ajito and K. Torimitsu, *Lab Chip*, 2002, **2**, 11–14.

134 S. Roy, H.-Y. Lin, C.-Y. Chou, C.-H. Huang, J. Small, N. Sadik, C. M. Ayinon, E. Lansbury, L. Cruz, A. Yekula, P. S. Jones, L. Balaj and B. S. Carter, *Int. J. Mol. Sci.*, 2019, **20**, 1349.

135 C. M. Hoo, N. Starostin, P. West and M. L. Mecartney, *J. Nanopart. Res.*, 2008, **10**, 89–96.

136 S. Atay, C. Gercel-Taylor, M. Kesimer and D. D. Taylor, *Exp. Cell Res.*, 2011, **317**, 1192–1202.

137 C. Gercel-Taylor, S. Atay, R. H. Tullis, M. Kesimer and D. D. Taylor, *Anal. Biochem.*, 2012, **428**, 44–53.

138 E. van der Pol, F. Coumans, Z. Varga, M. Krumrey and R. Nieuwland, *J. Thromb. Haemostasis*, 2013, **11**, 36–45.

139 S. Gurunathan, M.-H. Kang, M. Jeyaraj, M. Qasim and J.-H. Kim, *Cells*, 2019, **8**, 307.

140 G. Bryant and J. C. Thomas, *Langmuir*, 1995, **11**, 2480–2485.

141 S. Sharma, H. I. Rasool, V. Palanisamy, C. Mathisen, M. Schmidt, D. T. Wong and J. K. Gimzewski, *ACS Nano*, 2010, **4**, 1921–1926.

142 B. György, K. Módos, É. Pállinger, K. Pálóczi, M. Pásztói, P. Misják, M. A. Deli, Á. Sipos, A. Szalai, I. Voszka, A. Polgár, K. Tóth, M. Csete, G. Nagy, S. Gay, A. Falus, Á. Kittel and E. I. Buzás, *Blood*, 2011, **117**, e39–e48.

143 S. Sharma, F. Zuñiga, G. E. Rice, L. C. Perrin, J. D. Hooper and C. Salomon, *Oncotarget*, 2017, **8**, 104687–104703.

144 G. Binnig, C. F. Quate and C. Gerber, *Phys. Rev. Lett.*, 1986, **56**, 930–933.

145 Y. Yuana, T. H. Oosterkamp, S. Bahatyrova, B. Ashcroft, P. Garcia Rodriguez, R. M. Bertina and S. Osanto, *J. Thromb. Haemostasis*, 2010, **8**, 315–323.

146 J. Lötvall, A. F. Hill, F. Hochberg, E. I. Buzás, D. Di Vizio, C. Gardiner, Y. S. Gho, I. V. Kurochkin, S. Mathivanan, P. Quesenberry, S. Sahoo, H. Tahara, M. H. Wauben, K. W. Witwer and C. Théry, *J. Extracell. Vesicles*, 2014, **3**, 26913.

147 B. T. Pan, K. Teng, C. Wu, M. Adam and R. M. Johnstone, *J. Cell Biol.*, 1985, **101**, 942–948.

148 C. Harding, J. Heuser and P. Stahl, *J. Cell Biol.*, 1983, **97**, 329–339.

149 M. Colombo, G. Raposo and C. Théry, *Annu. Rev. Cell Dev. Biol.*, 2014, **30**, 255–289.

150 A. A. I. Sina, R. Vaidyanathan, A. Wuethrich, L. G. Carrascosa and M. Trau, *Anal. Bioanal. Chem.*, 2019, **411**, 1311–1318.

151 S. Picciolini, A. Gualerzi, R. Vanna, A. Sguassero, F. Gramatica, M. Bedoni, M. Masserini and C. Morasso, *Anal. Chem.*, 2018, **90**, 8873–8880.

152 L. Grasso, R. Wyss, L. Weidenauer, A. Thampi, D. Demurtas, M. Prudent, N. Lion and H. Vogel, *Anal. Bioanal. Chem.*, 2015, **407**, 5425–5432.

153 T. Vagner, A. Chin, J. Mariscal, S. Bannykh, D. M. Engman and D. Di Vizio, *Proteomics*, 2019, **19**, 1800167.

154 M. D. Lancé, Y. M. C. Henskens, P. Nelemans, M. H. S. Theunissen, R. V. Oerle, H. M. Spronk and M. A. E. Marcus, *Platelets*, 2013, **24**, 275–281.

155 J. Satsangi, D. P. Jewell, K. Welsh, M. Bunce and J. I. Bell, *Lancet*, 1994, **343**, 1509–1510.

156 C. A. Maguire, L. Balaj, S. Sivaraman, M. H. W. Crommentuijn, M. Ericsson, L. Mincheva-Nilsson, V. Baranov, D. Gianni, B. A. Tannous, M. Sena-Esteves, X. O. Breakefield and J. Skog, *Mol. Ther.*, 2012, **20**, 960–971.

157 M. D. Shah, A. L. Bergeron, J.-F. Dong and J. A. López, *Platelets*, 2008, **19**, 365–372.

158 R. E. Lane, D. Korbie, W. Anderson, R. Vaidyanathan and M. Trau, *Sci. Rep.*, 2015, **5**, 7639.

159 S. H. van Ierssel, E. M. Van Craenenbroeck, V. M. Conraads, V. F. Van Tendeloo, C. J. Vrints, P. G. Jorens and V. Y. Hoymans, *Thromb. Res.*, 2010, **125**, 332–339.

160 B. Shao and Z. Xiao, *Anal. Chim. Acta*, 2020, **1114**, 74–84.

161 X. Doldán, P. Fagúndez, A. Cayota, J. Laíz and J. P. Tosar, *Anal. Chem.*, 2016, **88**, 10466–10473.

162 J. Li, A. Wuethrich, S. Dey, R. E. Lane, A. A. I. Sina, J. Wang, Y. Wang, S. Puttick, K. M. Koo and M. Trau, *Adv. Funct. Mater.*, 2020, **30**, 1909306.

163 D. Feng, W.-L. Zhao, Y.-Y. Ye, X.-C. Bai, R.-Q. Liu, L.-F. Chang, Q. Zhou and S.-F. Sui, *Traffic*, 2010, **11**, 675–687.

164 A. E. Morelli, A. T. Larregina, W. J. Shufesky, M. L. G. Sullivan, D. B. Stolz, G. D. Papworth, A. F. Zahorchak, A. J. Logar, Z. Wang, S. C. Watkins, L. D. Falo Jr. and A. W. Thomson, *Blood*, 2004, **104**, 3257–3266.